



Intercomparison of Mobility Particle Size Spectrometers

Project No.:

Principal Investigator: Uta Wolf-Benning

Home Institution: Flughafen Berlin Brandenburg GmbH

Participant: Uta Wolf-Benning, Sebastian Aust, Lothar Keck

Candidate: **DE-FBB-WRAS 1**

Made by:

Counter (SN): GRIMM 5.420, SN: 54201608

Software: GRIMM

Candidate: **DE-FBB-WRAS 2**

Made by:

Counter (SN): GRIMM 5.420, SN: 54201607

Software: GRIMM

Location of the quality assurance: TROPOS Leipzig, lab 118

Comparison period: July 17, 2017 – July 21, 2017

Last Intercomparison (with Project No.):

Summary:

The airport Berlin Brandenburg participated with two GRIMM MPSS between July 17 to 21, 2017 in TROPOS. The goal was to characterise, understand and optimise the instruments for a future project. Participants were Uta Wolf-Benning and Sebastian Aust from airport Berlin and Lothar Keck from GRIMM. All results are documented in 5 night runs. All setup changes were discussed in the round. The data evaluation was done using both software versions of GRIMM and TROPOS. Each night is documented. Here are 3 important outputs:

1. PSL-measurements: TROPOS used 203 nm Latex particles. Both GRIMM MPSS systems showed a slightly higher diameter at 208 nm. The sheath air is controlled by an internal critical orifice and can't be adjusted. This shift can be seen in the size distribution compared with the

- 1 -

TROPOS Reference Instrument. Examples are shown in the measurements from 18.-19.07.2017.

2. CPC-Efficiency curve: Referring to the CPC workshop report, we used the GRIMM software to determine the CPC-efficiency curve. TROPOS recommends FBB to do a second CPC workshop with BNC pulse output. Using the measured efficiency curve in the data evaluation, we overestimate the aiten- and accumulation mode particles.
3. To understand the different data evaluation steps, we evaluated the raw data separately with GRIMM and TROPOS softwares. The multiple charge inversion showed no significant differences. However, looking at the diffusion loss correction, there are significant differences observed. To get a clear picture off all diffusion losses, we measured the effective lengths for each setup and made a sketch. If we add these corrections to the inverted data, the GRIMM MPSS fits better to the Reference Instrument. That means the GRIMM software underestimates the diffusion losses. TROPOS recommends to do a separate offline calculation for the diffusion losses.

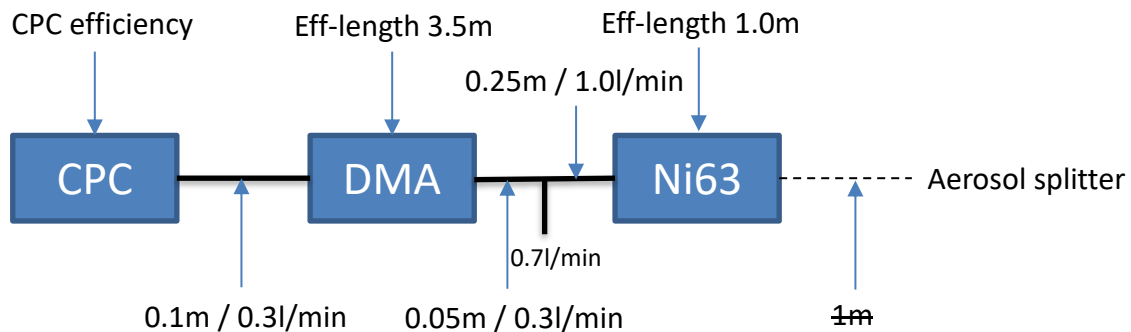
The check of both instruments during the whole week was quite complex and showed different results depending on the setup. For detailed information, look at the results for each night. Using the correct setup and data evaluation processes for both GRIMM systems, results are in the range of +/-10% of the Reference Instrument. In this case, the GRIMM systems passed the quality standards of ACTRIS and GAW.

Information about the instruments: TROPOS MPSS

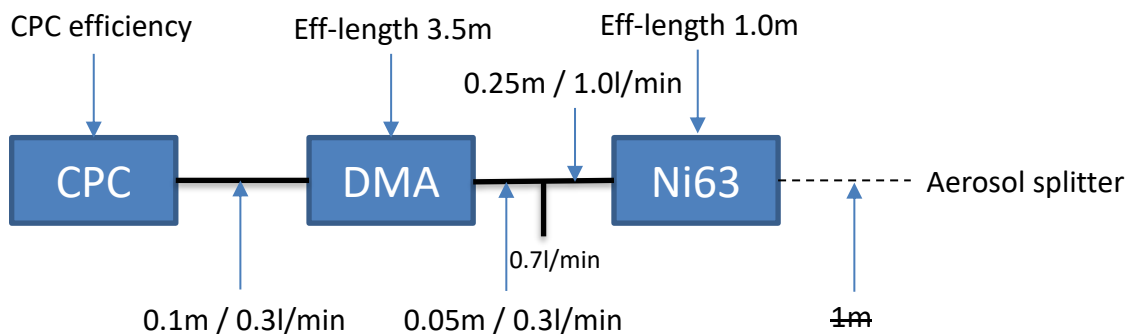
List of Components	TROPOS Reference MPSS No.1	DE-FBB-WRAS 1	DE-FBB-WRAS 2
Position	Line 1	Line 1	Line 1
Company	TROPOS	GRIMM	GRIMM
Software	TROPOS	GRIMM	GRIMM
CPC-MPSS	TSI CPC, Model 3772	GRIMM, Model 5.420	GRIMM, Model 5.420
CPC-total	TSI CPC, Model 3010	-	-
flow ratio	1.0 : 5.0	0.3 : 3.0	0.3 : 3.0
source	Kr85	Ni63	Ni63
HV power supply	Positive	positive	positive
DMA	Hauke medium	GRIMM	GRIMM
aerosol dryer	✓		
aerosol RH- sensor	✓		
aerosol T-sensor	✓		
sheath RH-sensor	✓	-	-
sheath T-sensor	✓	-	-
Sheath dryer	✓	-	-
pressure sensor	✓	✓	✓
info		-	GRIMM-Inlet with dryer

Information to the setup and legend:

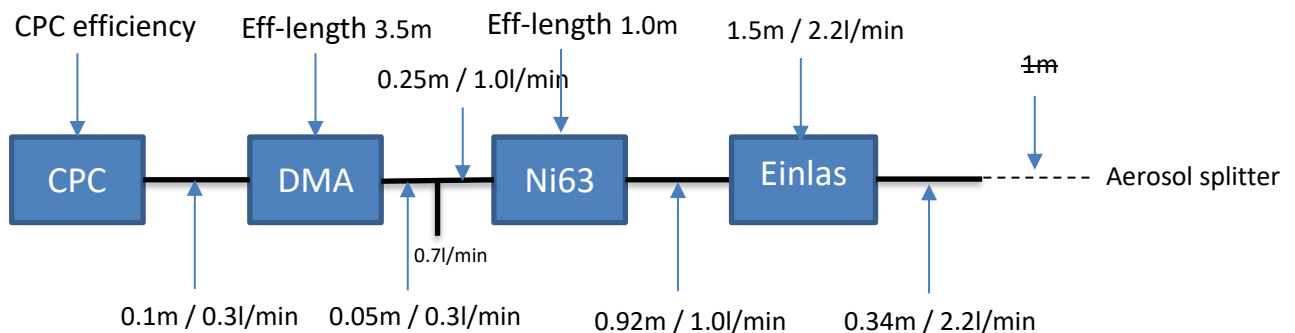
WRAS 1/2



WRAS 1 spezial



WRAS 2 with inlet



Legend for the data evaluation	Short cut	corrections	info
Block 1: GRIMM Software	G_raw	-	
	G_inv	MLI	0.3 : 3.0
	G_in1	MLI + DMA	
	G_in3	MLI + DMA + CPC	
Block 2: TROPOS Software	G_raw	-	
	T_inv	MLI	0.3 : 3.0
	T_in1	MLI + DMA	
	T_in2	MLI + DMA + Diff	
	T_in3	MLI + DMA + Diff + CPC	
	T_in4	MLI + DMA + Diff + CPC + Inlet	
	T_in5	MLI + DMA + Diff + Inlet	
Block 3: Kombination aus GRIMM & TROPOS	G_inv	MLI	0.3 : 3.0
	GT_in1	MLI + DMA	
	GT_in2	MLI + DMA + Diff	
	GT_in3	MLI + DMA + Diff + CPC	
	GT_in4	MLI + DMA + Diff + CPC + Inlet	
	GT_in5	MLI + DMA + Diff + Inlet	

G: GRIMM evaluation

T: TROPOS evaluation

GT: Combination of GRIMM and TROPOS evaluation

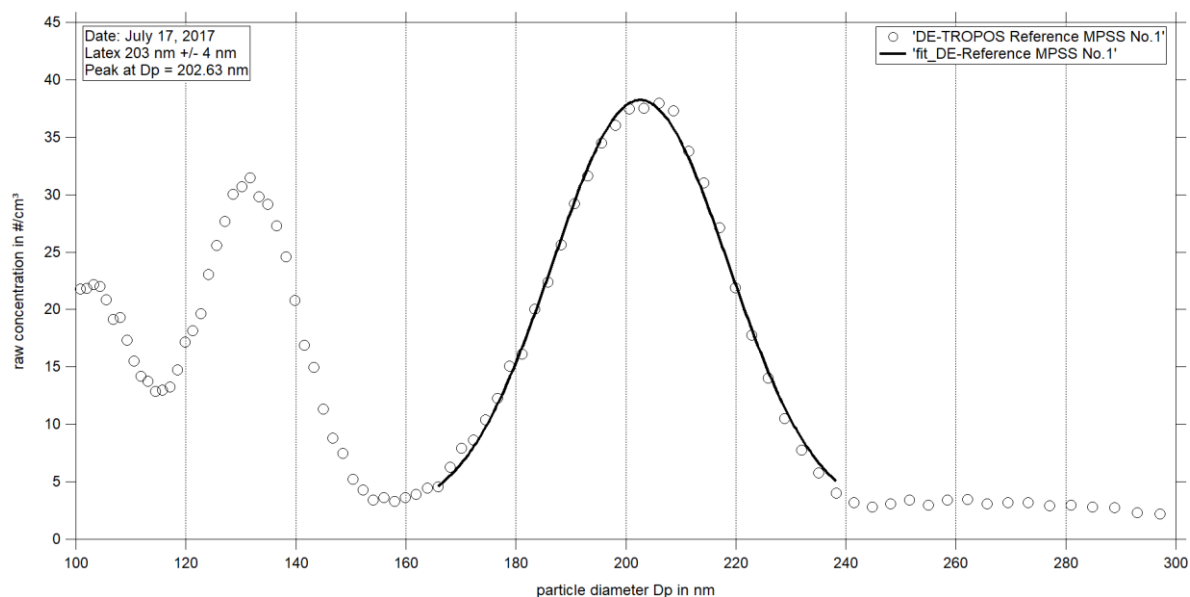
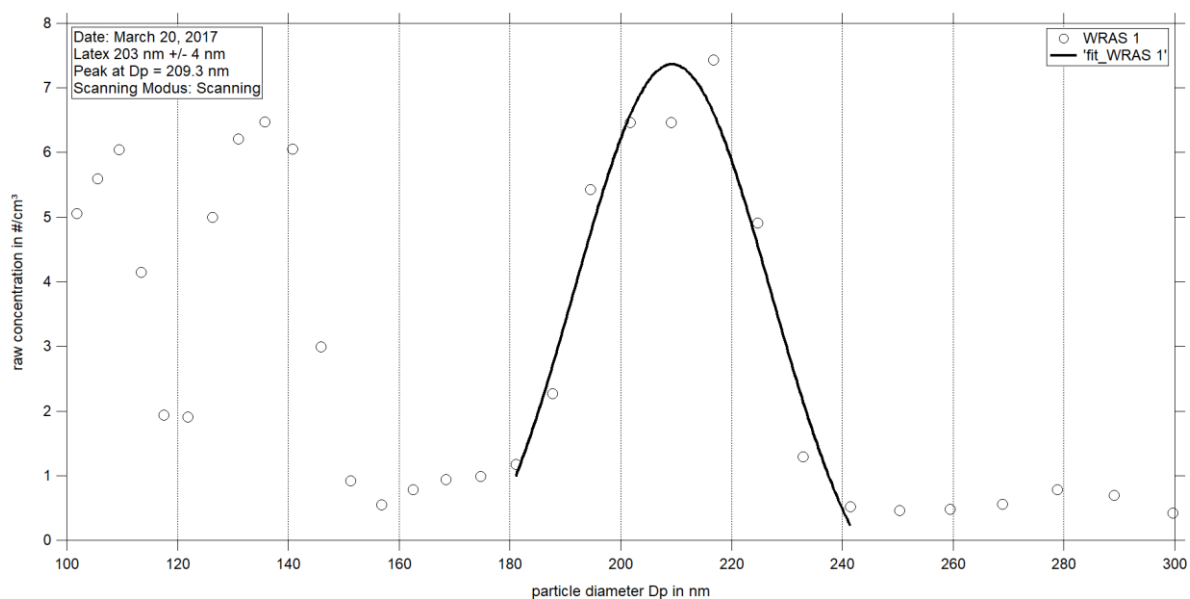
MLI: Multiple Charge Inversion

DMA: Diffusion loss corrections in the DMA (effective length)

Diff: Diffusion loss corrections in the system (effective length)

CPC: CPC Efficiency Curve

Inlet: Diffusion loss corrections in the inlet (effective length)

PSL Scan and calibration: Latex 203 nm +/- 4 nm**Figure 01:** Measurement of latex 203 nm: Particle size distribution (raw concentration) for latex 203 nm on June 17th, 2017.**Figure 02:** Measurement of latex 203 nm: Particle size distribution (raw concentration) for latex 203 nm on July 20th, 2017.

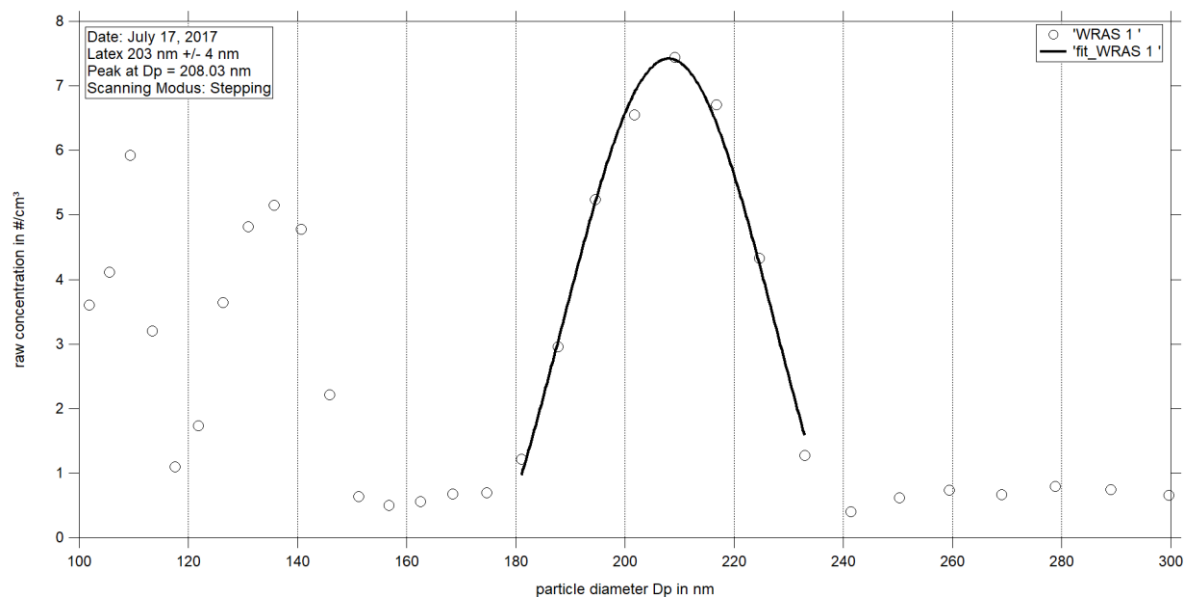


Figure 03: Measurement of latex 203 nm: Particle size distribution (raw concentration) for latex 203 nm on July 17rd, 2017.

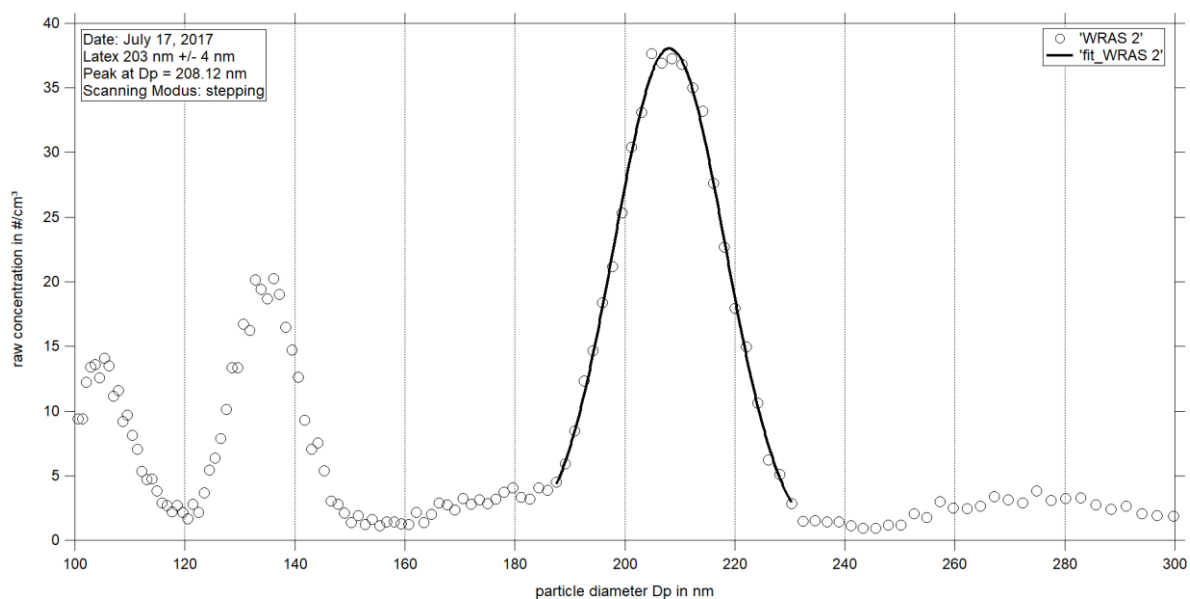


Figure 04: Measurement of latex 203 nm: Particle size distribution (raw concentration) for latex 203 nm on July 17rd, 2017.

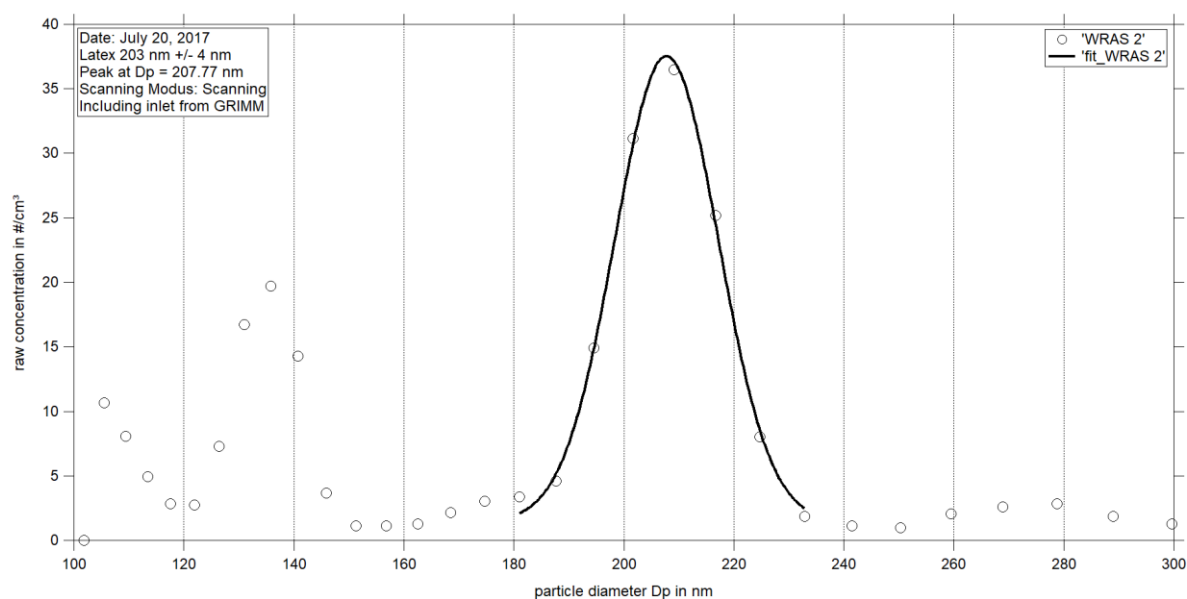


Figure 05: Measurement of latex 203 nm: Particle size distribution (raw concentration) for latex 203 nm on July 20th, 2017. The settings of the WRAS 2 was “scanning” including the inlet.

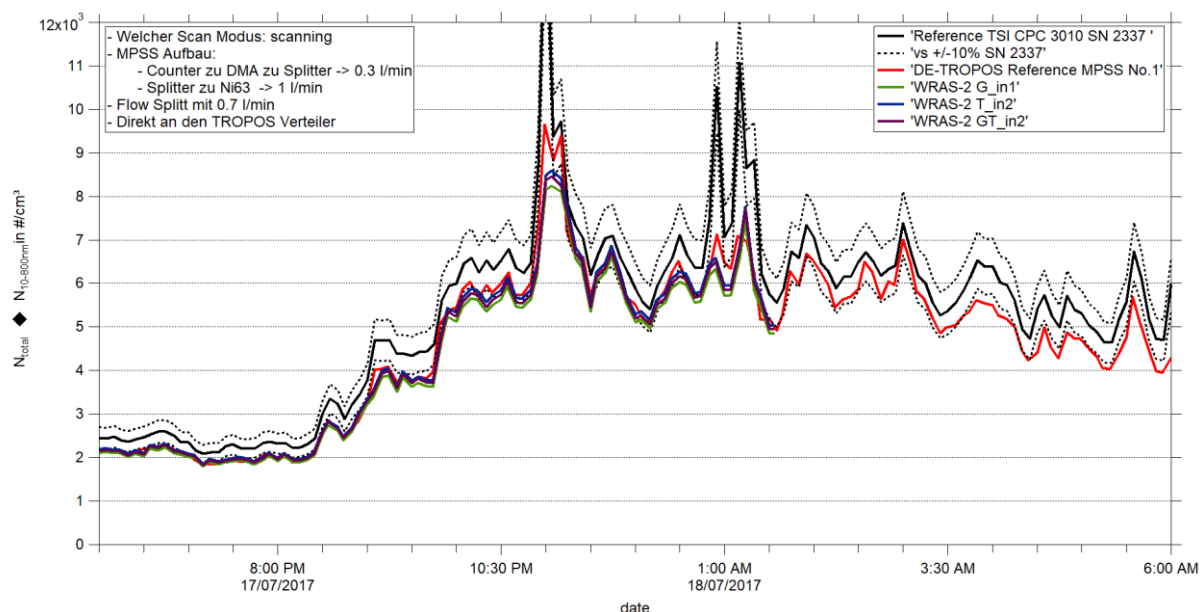
NIGHT: 17. - 18.07.2017

Figure 06: Time series (July 17, 2017 06:00 PM – July 18, 2017 06:00 AM) of the integrated particle number concentration ($N_{10-800nm}$) of the MPSS and total number concentration (N_{total}) of the Reference TSI-CPC Model 3010. The inversion for the candidate was performed using TSI and TROPOS software. Multiple charge correction, internal diffusion losses and CPC flow corrections are included by using different “ini” steps.

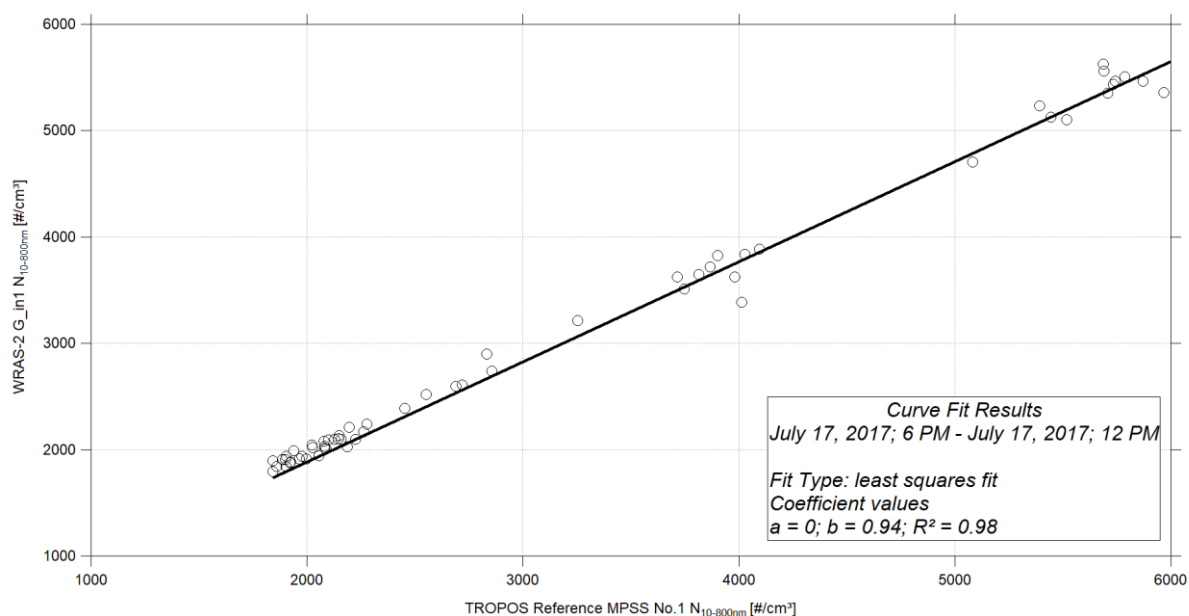


Figure 07: Linear regression between the number concentrations of the TROPOS Reference MPSS No.1 and WRAS-2 G_in1 (July 17, 2017 06:00 PM – July 18, 2017 06:00 AM). Multiple charge correction, internal diffusion losses and CPC flow corrections are included by using different “ini” steps.

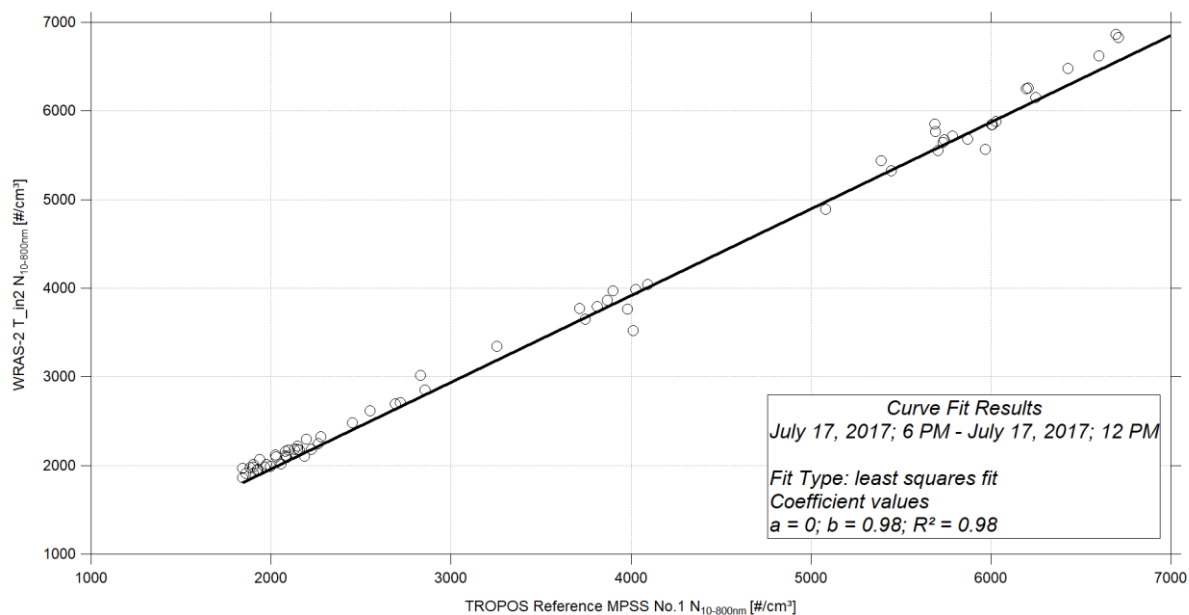


Figure 08: Linear regression between the number concentrations of the TROPOS Reference MPSS No.1 and WRAS-2 T_{in2} (July 17, 2017 06:00 PM – July 18, 2017 06:00 AM). Multiple charge correction, internal diffusion losses and CPC flow corrections are included by using different “ini” steps.

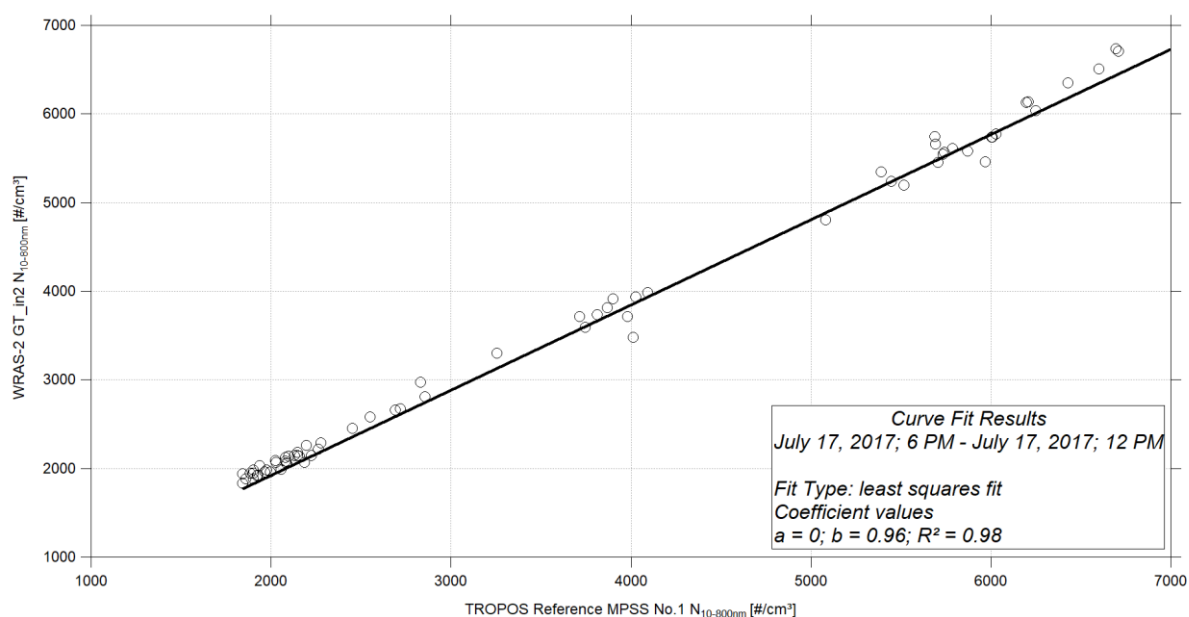


Figure 09: Linear regression between the number concentrations of the TROPOS Reference MPSS No.1 and WRAS-2 GT_{in2} (July 17, 2017 06:00 PM – July 18, 2017 06:00 AM). Multiple charge correction, internal diffusion losses and CPC flow corrections are included by using different “ini” steps.

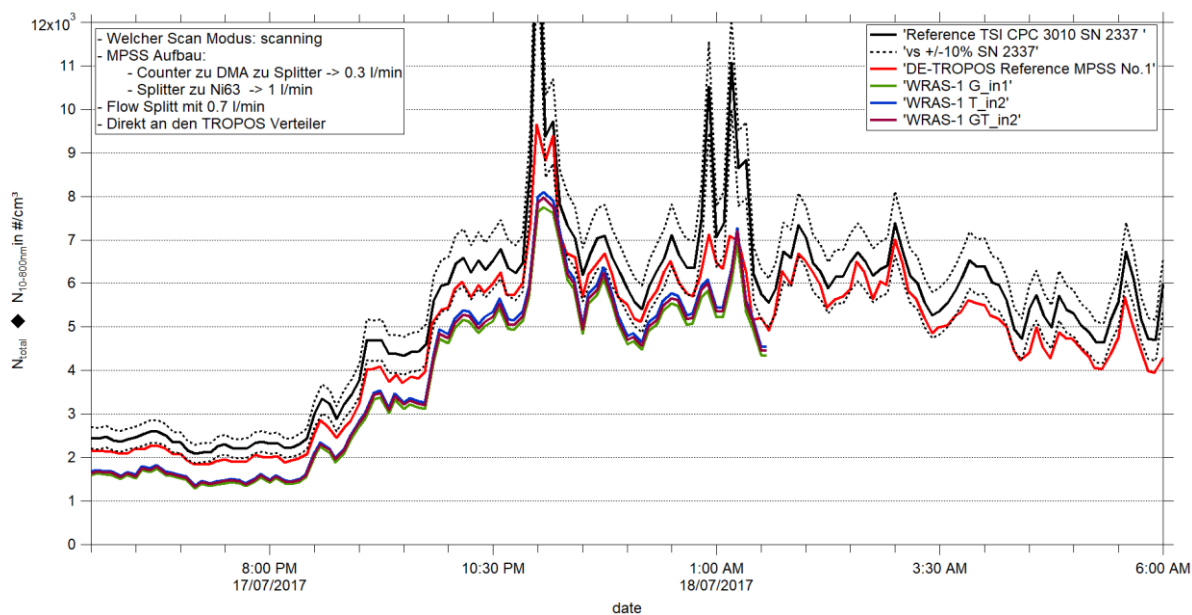


Figure 10: Time series (July 17, 2017 06:00 PM – July 18, 2017 06:00 AM) of the integrated particle number concentration ($N_{10-800nm}$) of the MPSS and total number concentration (N_{total}) of the Reference TSI-CPC Model 3010. The inversion for the candidate was performed using TSI and TROPOS software. Multiple charge correction, internal diffusion losses and CPC flow corrections are included by using different “ini” steps.

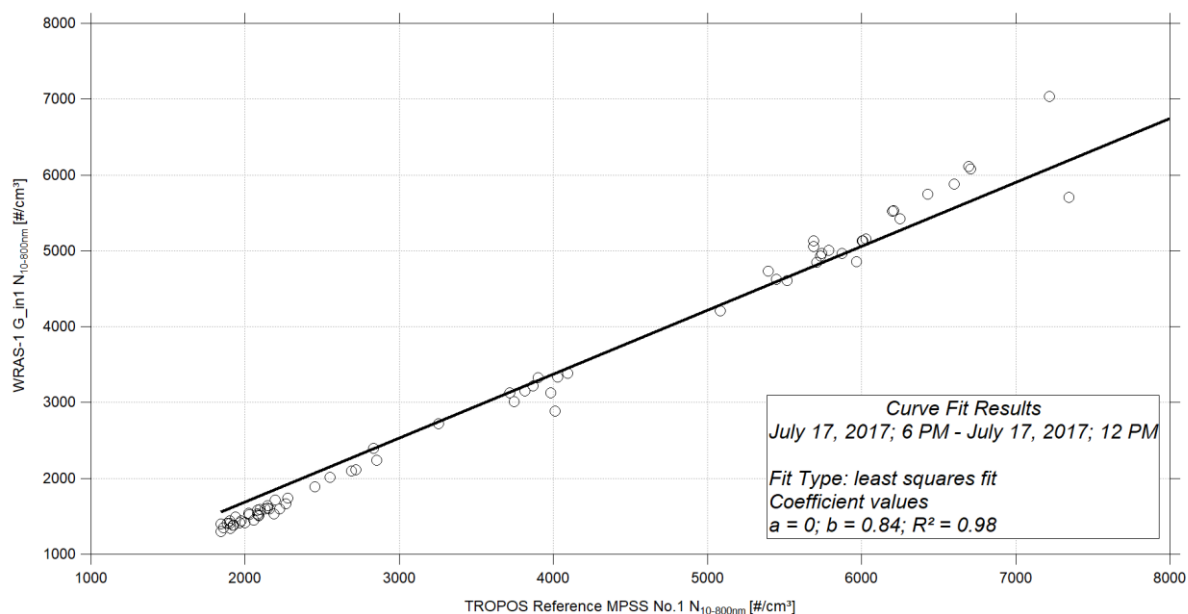


Figure 11: Linear regression between the number concentrations of the TROPOS Reference MPSS No.1 and WRAS-1 G_in1 (July 17, 2017 06:00 PM – July 18, 2017 06:00 AM). Multiple charge correction, internal diffusion losses and CPC flow corrections are included by using different “ini” steps.

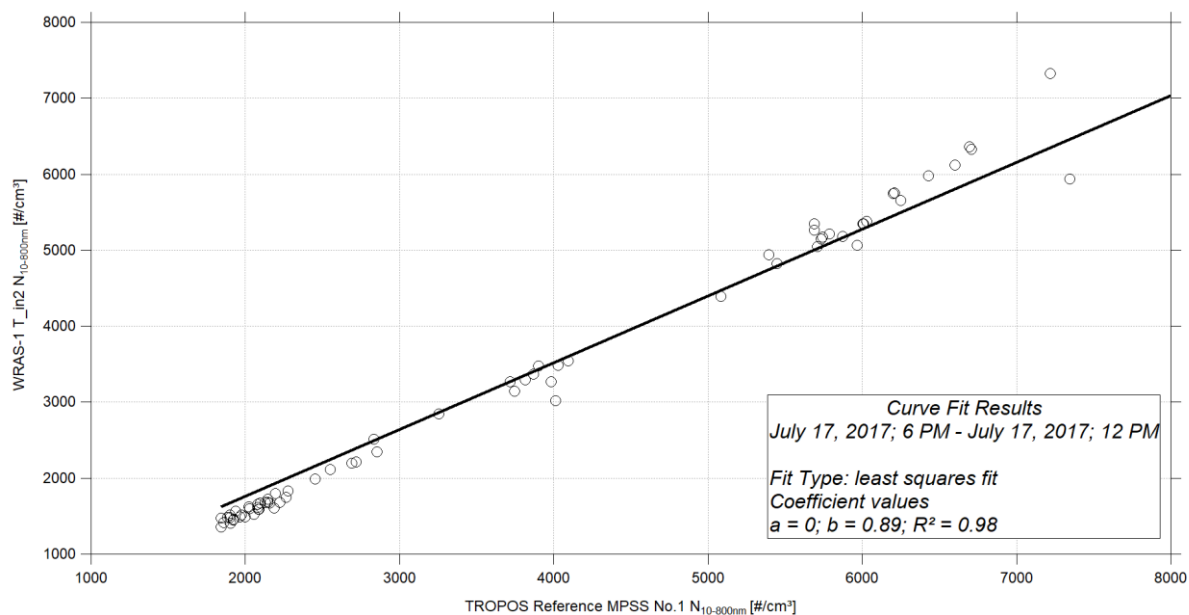


Figure 12: Linear regression between the number concentrations of the TROPOS Reference MPSS No.1 and WRAS-1 T_in2 (July 17, 2017 06:00 PM – July 18, 2017 06:00 AM). Multiple charge correction, internal diffusion losses and CPC flow corrections are included by using different “ini” steps.

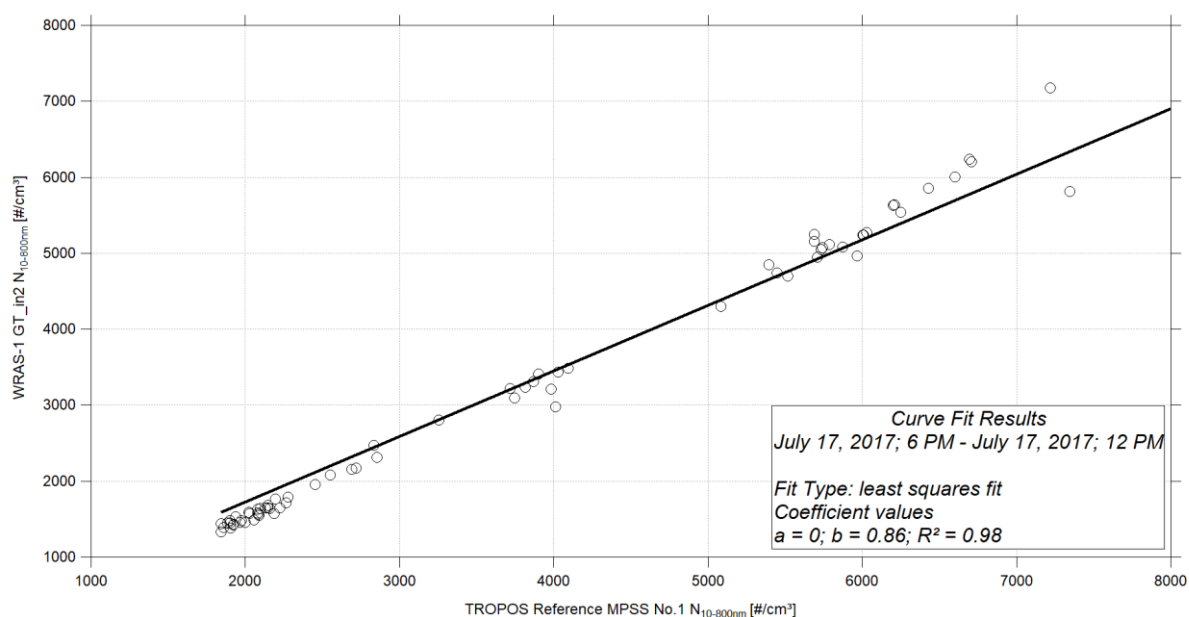


Figure 13: Linear regression between the number concentrations of the TROPOS Reference MPSS No.1 and WRAS-1 GT_in2 (July 17, 2017 06:00 PM – July 18, 2017 06:00 AM). Multiple charge correction, internal diffusion losses and CPC flow corrections are included by using different “ini” steps.

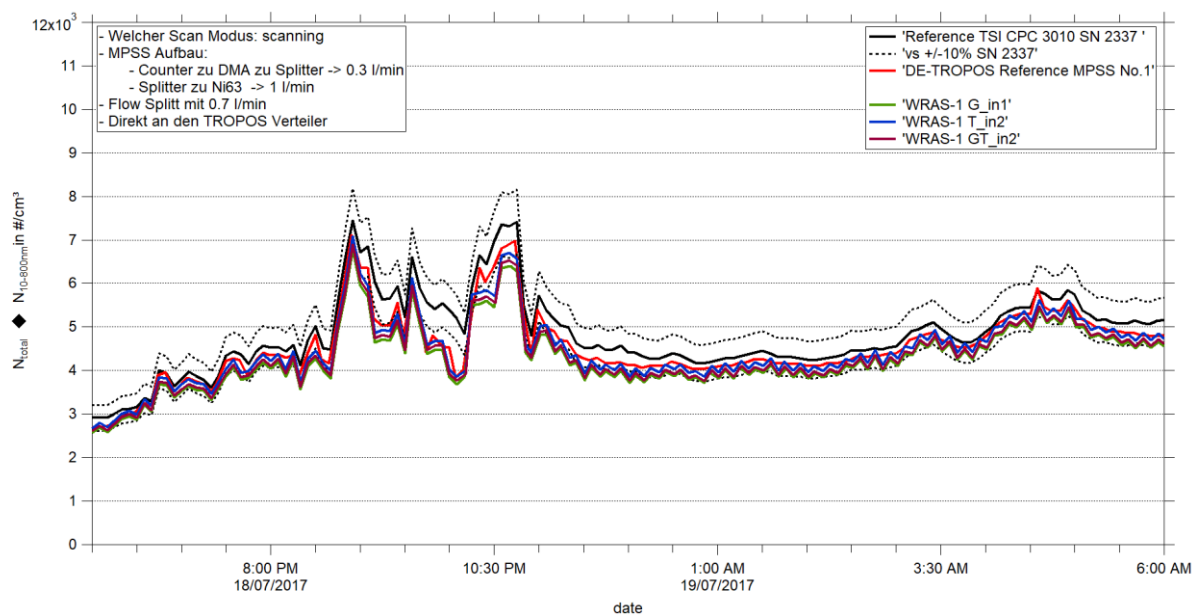
NIGHT: 18. - 19.07.2017

Figure 14: Time series (July 18, 2017 06:00 PM – July 19, 2017 06:00 AM) of the integrated particle number concentration ($N_{10-800nm}$) of the MPSS and total number concentration (N_{total}) of the Reference TSI-CPC Model 3010. The inversion for the candidate was performed using TSI and TROPOS software. Multiple charge correction, internal diffusion losses and CPC flow corrections are included by using different “ini” steps.

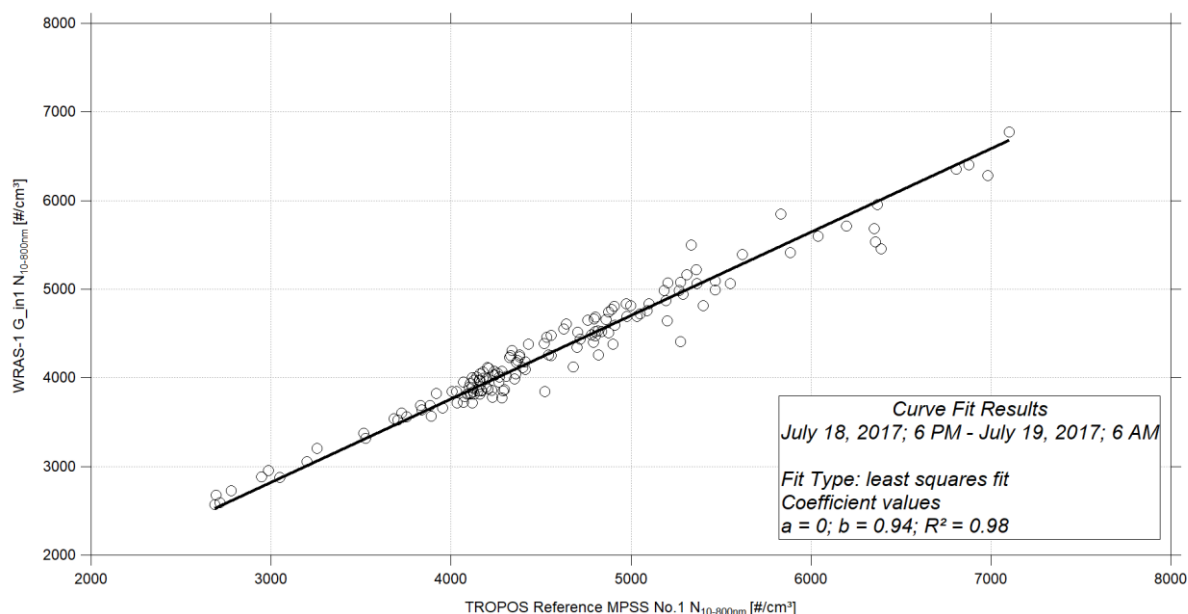


Figure 15: Linear regression between the number concentrations of the TROPOS Reference MPSS No.1 and WRAS-1 G_in1 (July 18, 2017 06:00 PM – July 19, 2017 06:00 AM). Multiple charge correction, internal diffusion losses and CPC flow corrections are included by using different “ini” steps.

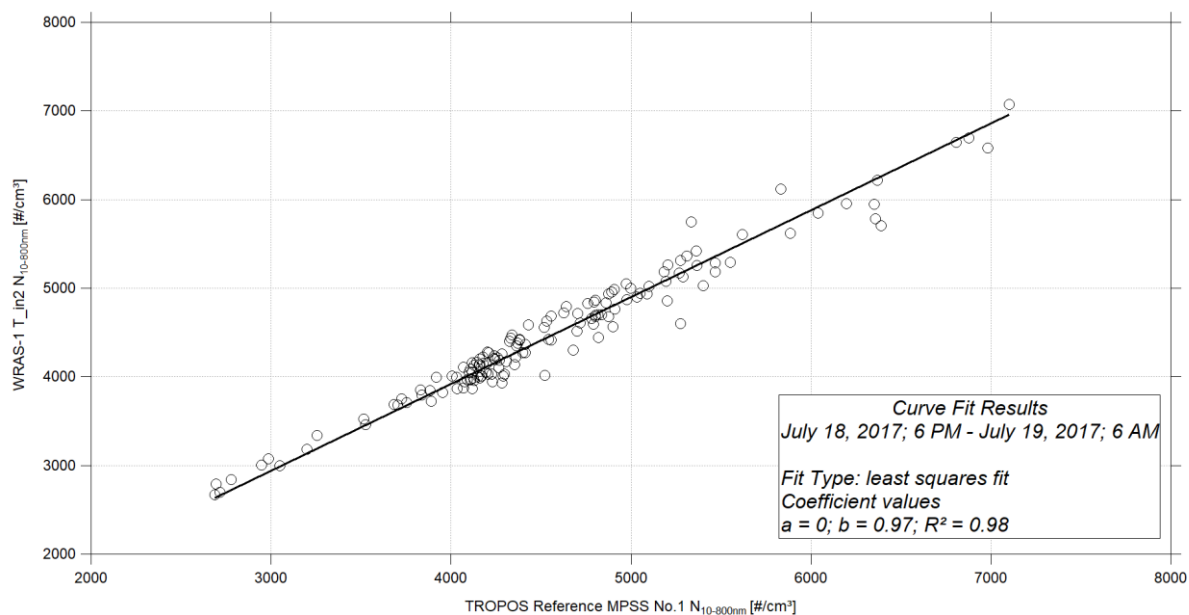


Figure 16: Linear regression between the number concentrations of the TROPOS Reference MPSS No.1 and WRAS-1 T_in2 (July 18, 2017 06:00 PM – July 19, 2017 06:00 AM). Multiple charge correction, internal diffusion losses and CPC flow corrections are included by using different “ini” steps.

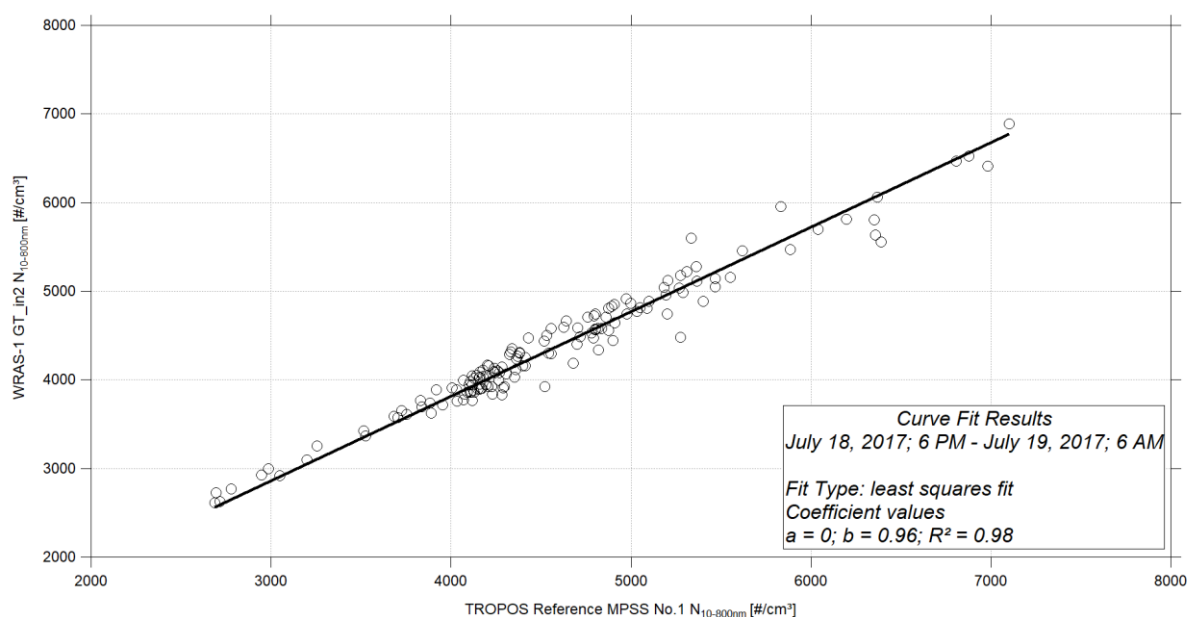


Figure 17: Linear regression between the number concentrations of the TROPOS Reference MPSS No.1 and WRAS-1 GT_in2 (July 18, 2017 06:00 PM – July 19, 2017 06:00 AM). Multiple charge correction, internal diffusion losses and CPC flow corrections are included by using different “ini” steps.

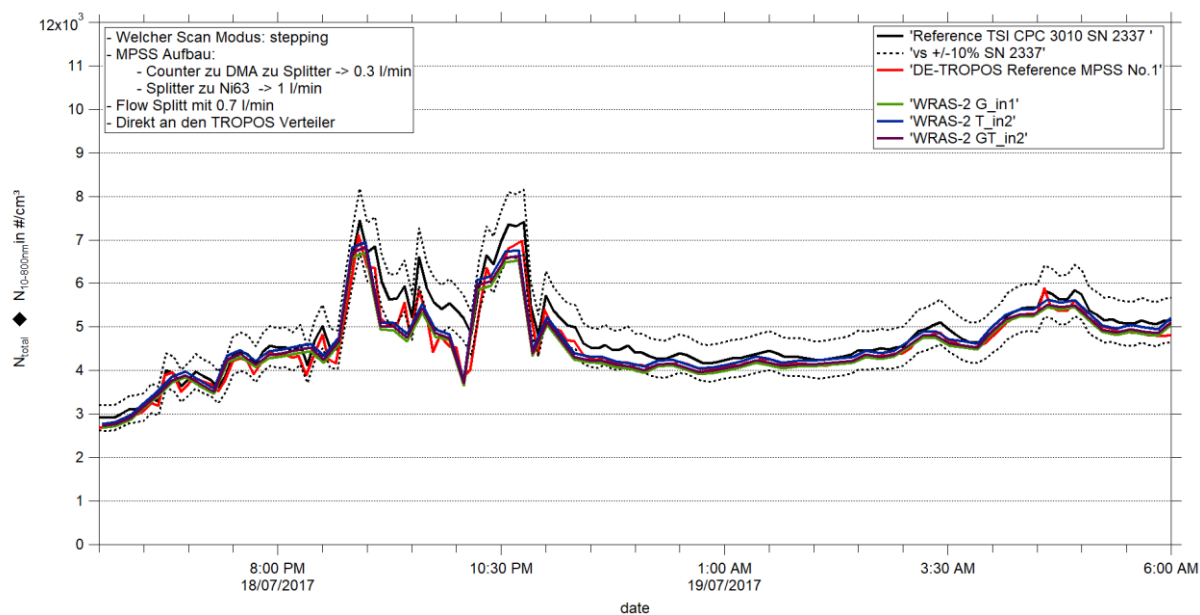


Figure 18: Time series (July 18, 2017 06:00 PM – July 19, 2017 06:00 AM) of the integrated particle number concentration ($N_{10-800nm}$) of the MPSS and total number concentration (N_{total}) of the Reference TSI-CPC Model 3010. The inversion for the candidate was performed using TSI and TROPOS software. Multiple charge correction, internal diffusion losses and CPC flow corrections are included by using different “ini” steps.

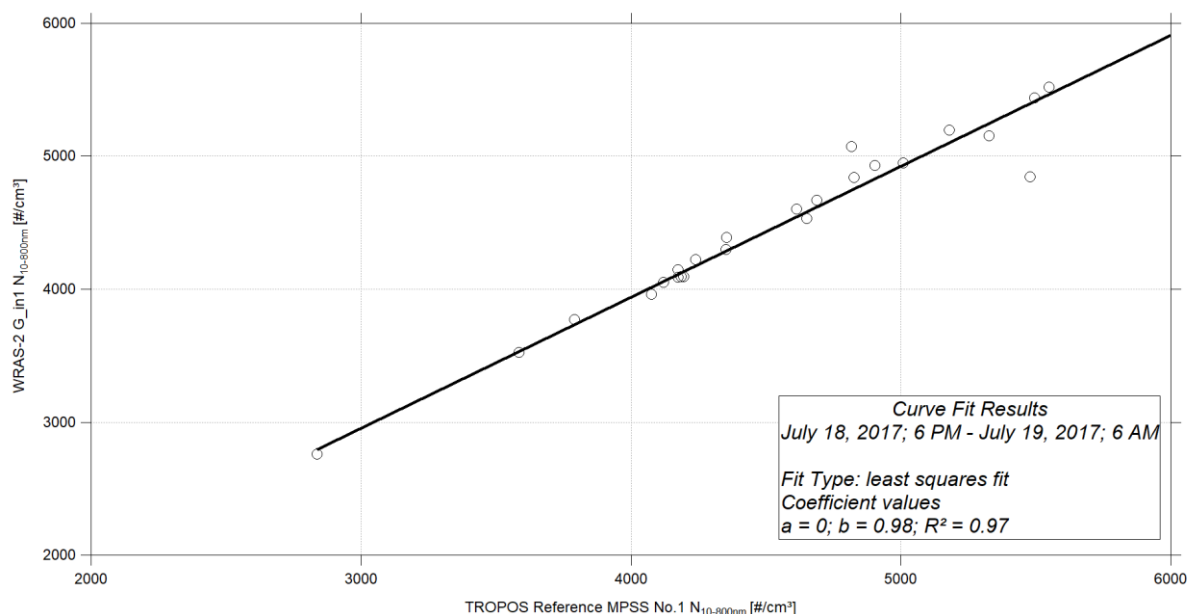


Figure 19: Linear regression between the number concentrations of the TROPOS Reference MPSS No.1 and WRAS-2 G_in1 (July 18, 2017 06:00 PM – July 19, 2017 06:00 AM). Multiple charge correction, internal diffusion losses and CPC flow corrections are included by using different “ini” steps.

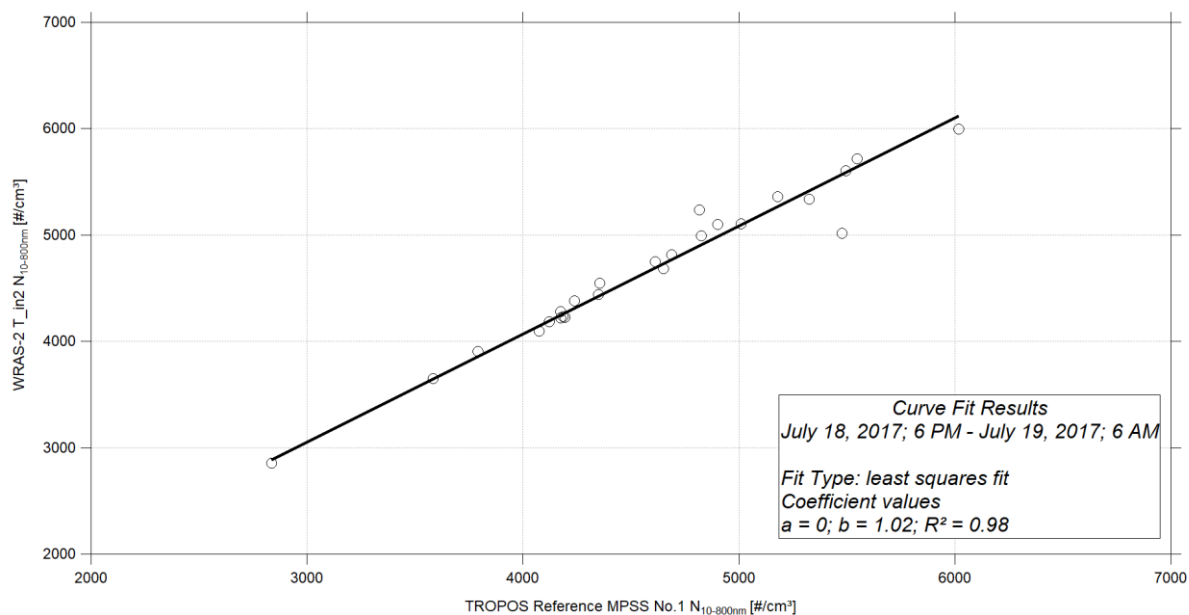


Figure 20: Linear regression between the number concentrations of the TROPOS Reference MPSS No.1 and WRAS-2 T_in2 (July 18, 2017 06:00 PM – July 19, 2017 06:00 AM). Multiple charge correction, internal diffusion losses and CPC flow corrections are included by using different “ini” steps.

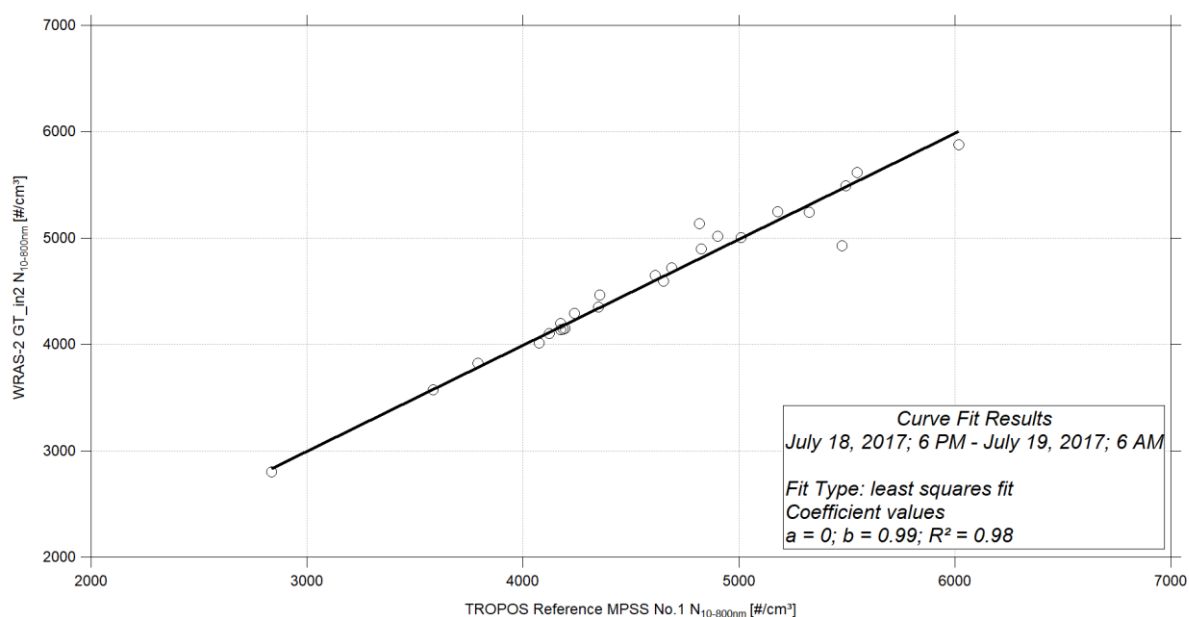


Figure 21: Linear regression between the number concentrations of the TROPOS Reference MPSS No.1 and WRAS-2 GT_in2 (July 18, 2017 06:00 PM – July 19, 2017 06:00 AM). Multiple charge correction, internal diffusion losses and CPC flow corrections are included by using different “ini” steps.

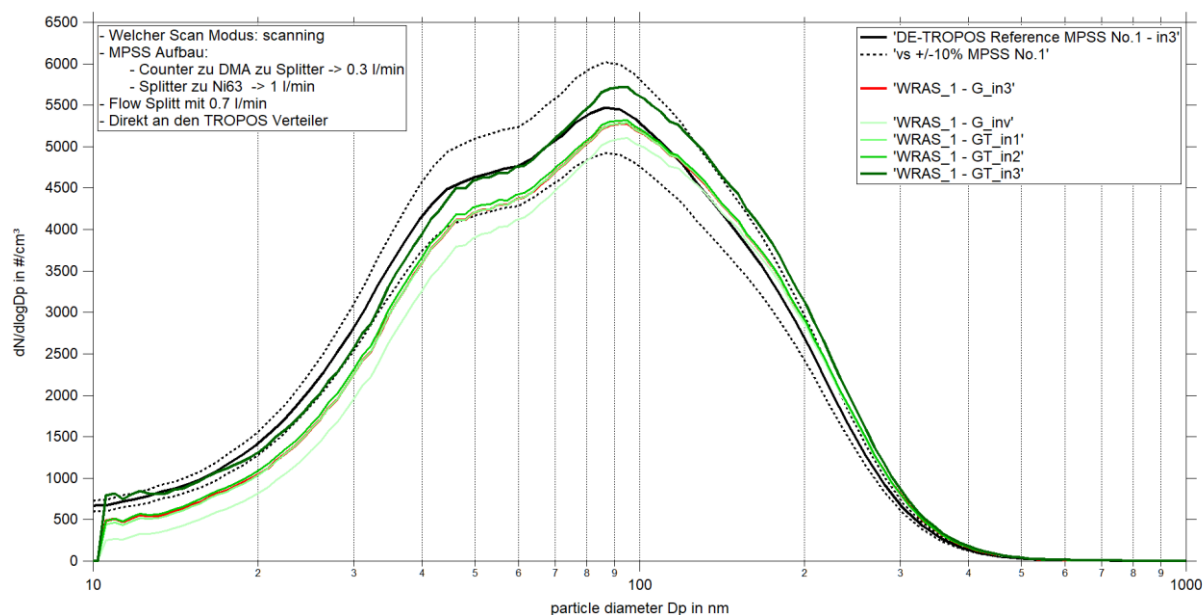


Figure 22: Comparison of mean particle number size distribution of TROPOS Reference MPSS No.1 against WRAS-1 from July 18, 2017 06:00 PM – July 19, 2017 06:00 AM. Multiple charge correction, internal diffusion losses and CPC efficiency are included by using different “ini” steps. Using GRIMM inversion and TROPOS corrections.

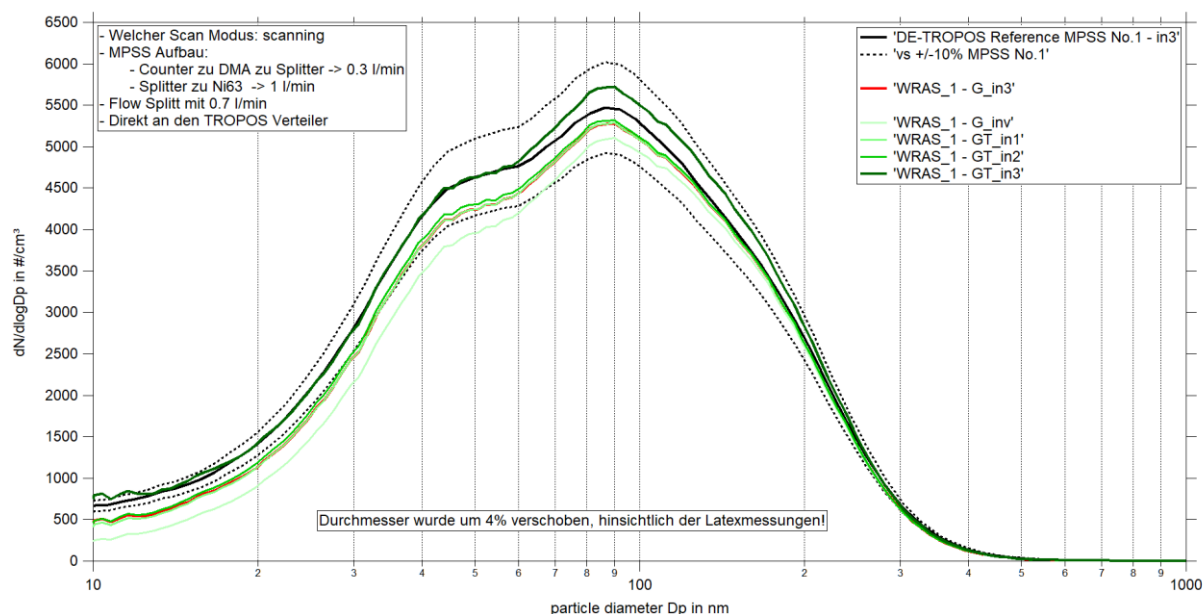


Figure 23: Comparison of mean particle number size distribution of TROPOS Reference MPSS No.1 against WRAS-1 from July 18, 2017 06:00 PM – July 19, 2017 06:00 AM. Multiple charge correction, internal diffusion losses and CPC efficiency are included by using different “ini” steps. Sizing shift by 4% because of the previous latex scans.

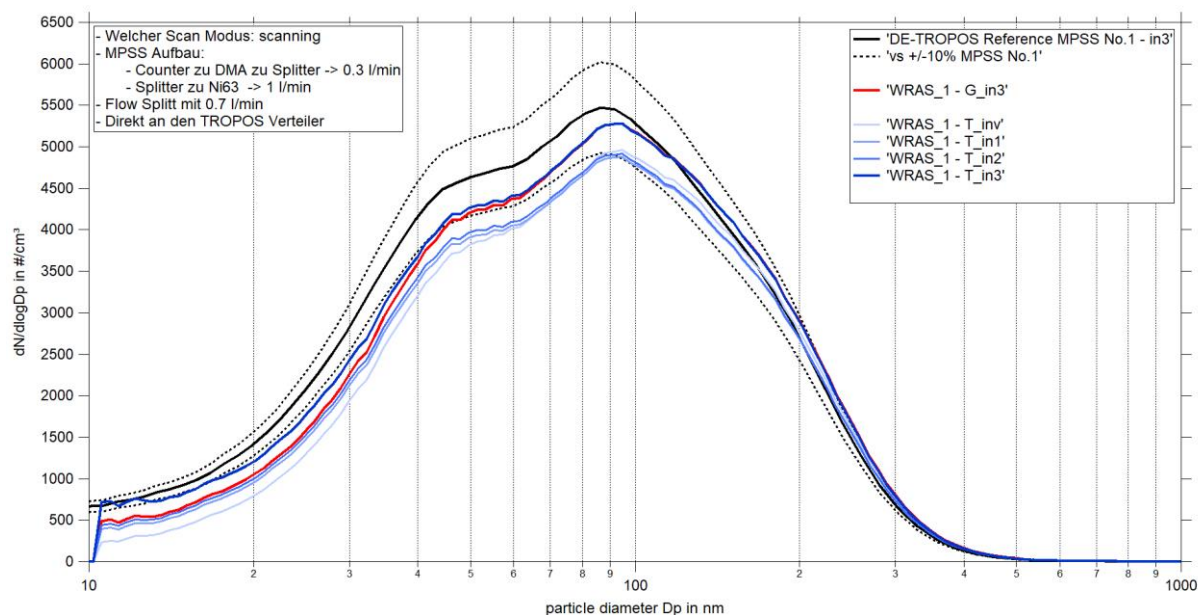


Figure 24: Comparison of mean particle number size distribution of TROPOS Reference MPSS No.1 against WRAS-1 from July 18, 2017 06:00 PM – July 19, 2017 06:00 AM. Multiple charge correction, internal diffusion losses and CPC efficiency are included by using different “ini” steps. Using only TROPOS inversion and corrections.

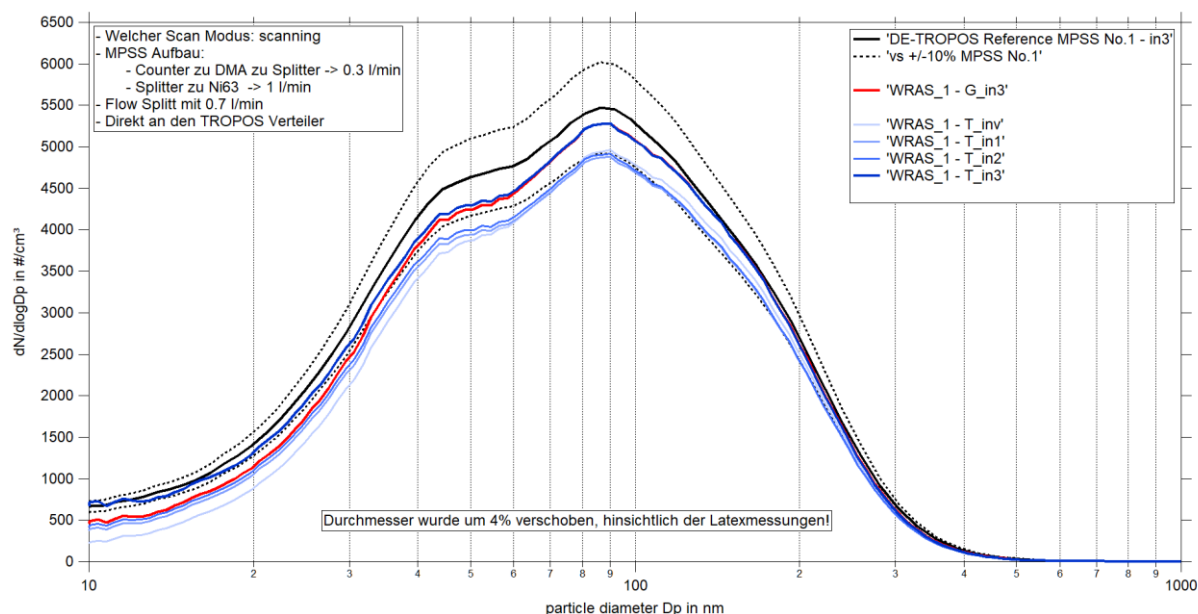


Figure 25: Comparison of mean particle number size distribution of TROPOS Reference MPSS No.1 against WRAS-1 from July 18, 2017 06:00 PM – July 19, 2017 06:00 AM. Multiple charge correction, internal diffusion losses and CPC efficiency are included by using different “ini” steps. Sizing shift by 4% because of the previous latex scans.

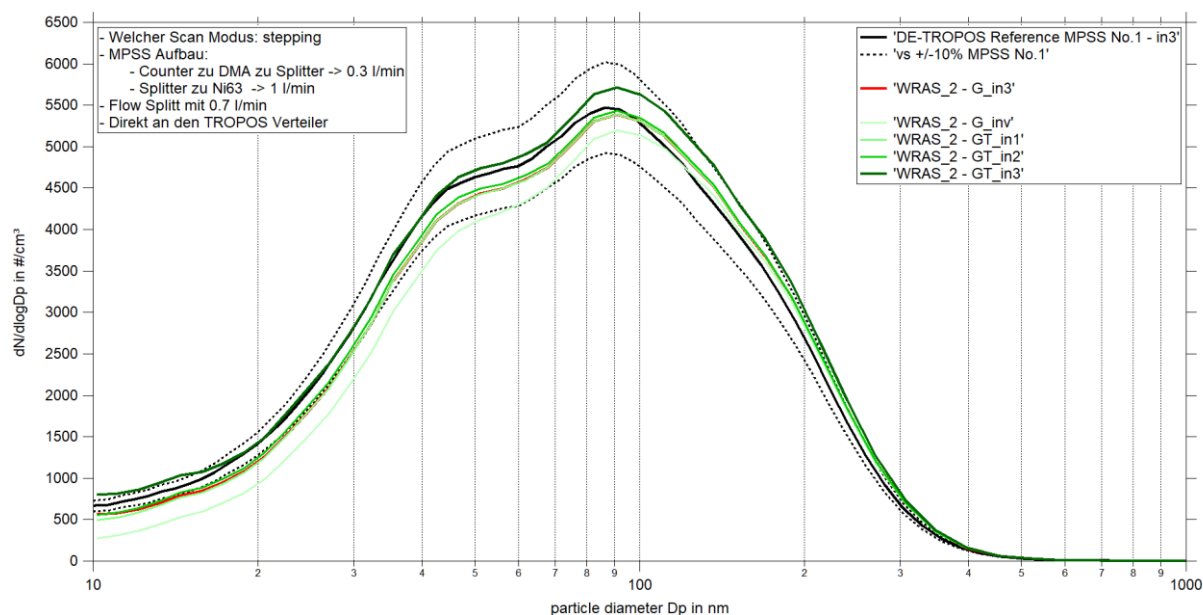


Figure 26: Comparison of mean particle number size distribution of TROPOS Reference MPSS No.1 against WRAS-2 from July 18, 2017 06:00 PM – July 19, 2017 06:00 AM. Multiple charge correction, internal diffusion losses and CPC efficiency are included by using different “ini” steps. Using GRIMM inversion and TROPOS corrections.

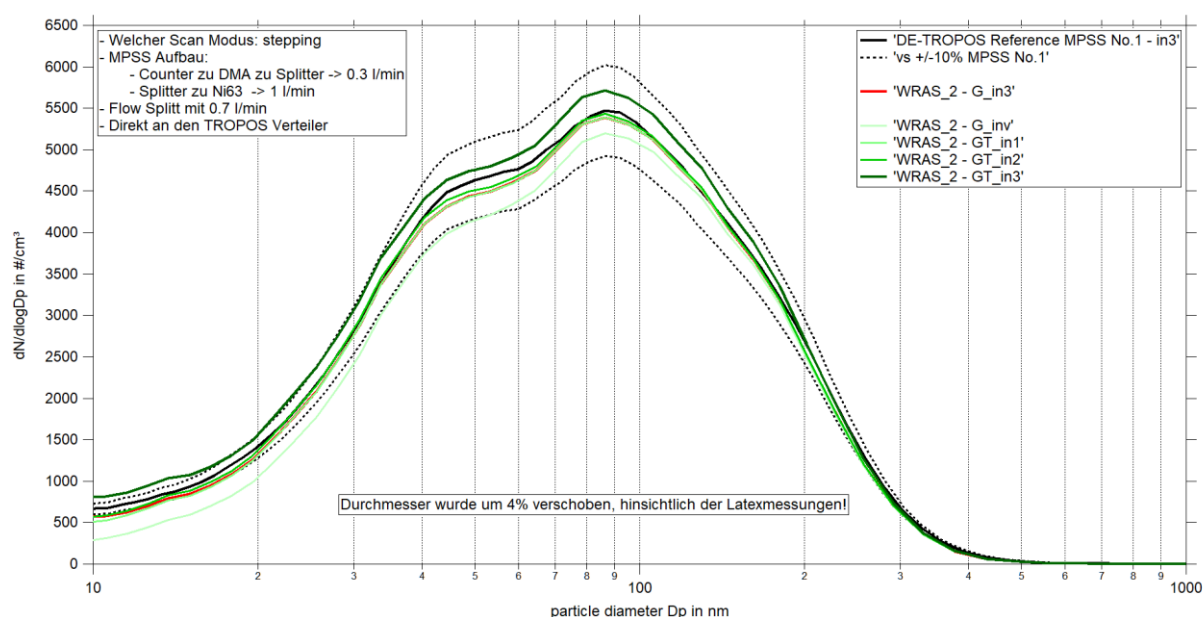


Figure 27: Comparison of mean particle number size distribution of TROPOS Reference MPSS No.1 against WRAS-2 from July 18, 2017 06:00 PM – July 19, 2017 06:00 AM. Multiple charge correction, internal diffusion losses and CPC efficiency are included by using different “ini” steps. Sizing shift by 4% because of the previous latex scans.

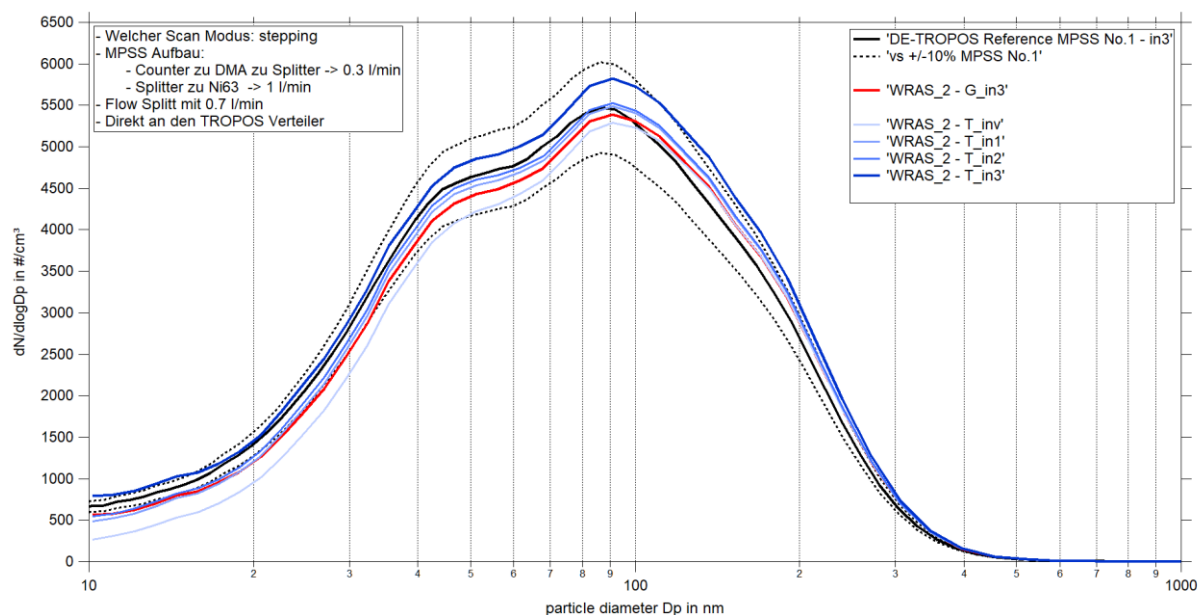


Figure 28: Comparison of mean particle number size distribution of TROPOS Reference MPSS No.1 against WRAS-2 from July 18, 2017 06:00 PM – July 19, 2017 06:00 AM. Multiple charge correction, internal diffusion losses and CPC efficiency are included by using different “ini” steps. Using only TROPOS inversion and corrections.

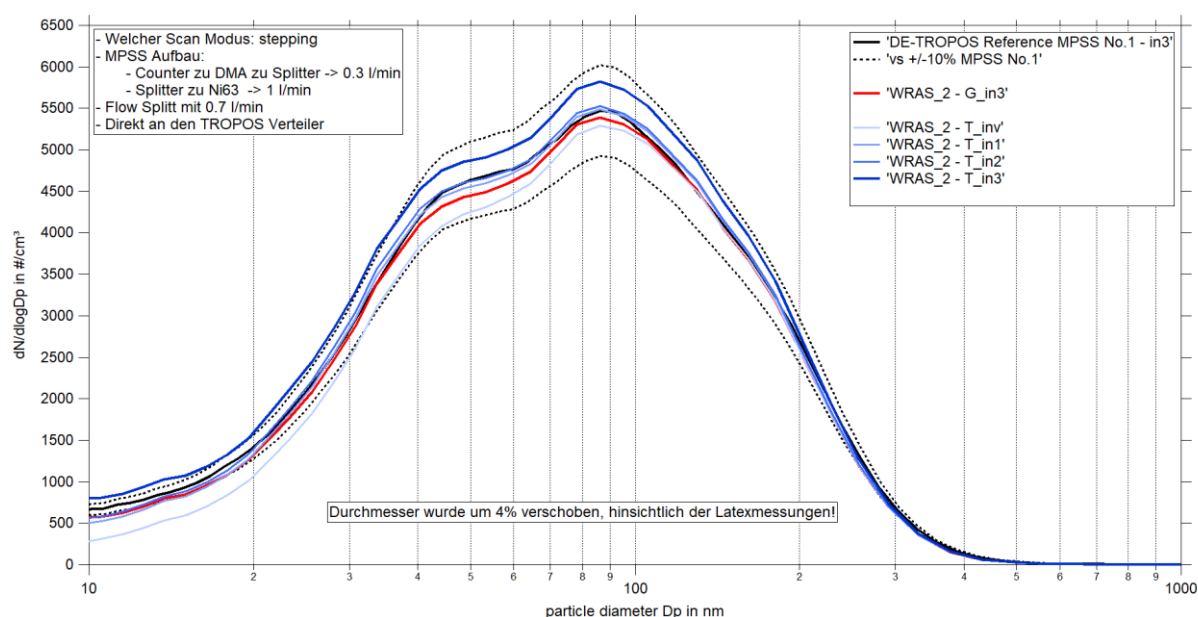


Figure 29: Comparison of mean particle number size distribution of TROPOS Reference MPSS No.1 against WRAS-2 from July 18, 2017 06:00 PM – July 19, 2017 06:00 AM. Multiple charge correction, internal diffusion losses and CPC efficiency are included by using different “ini” steps. Sizing shift by 4% because of the previous latex scans.

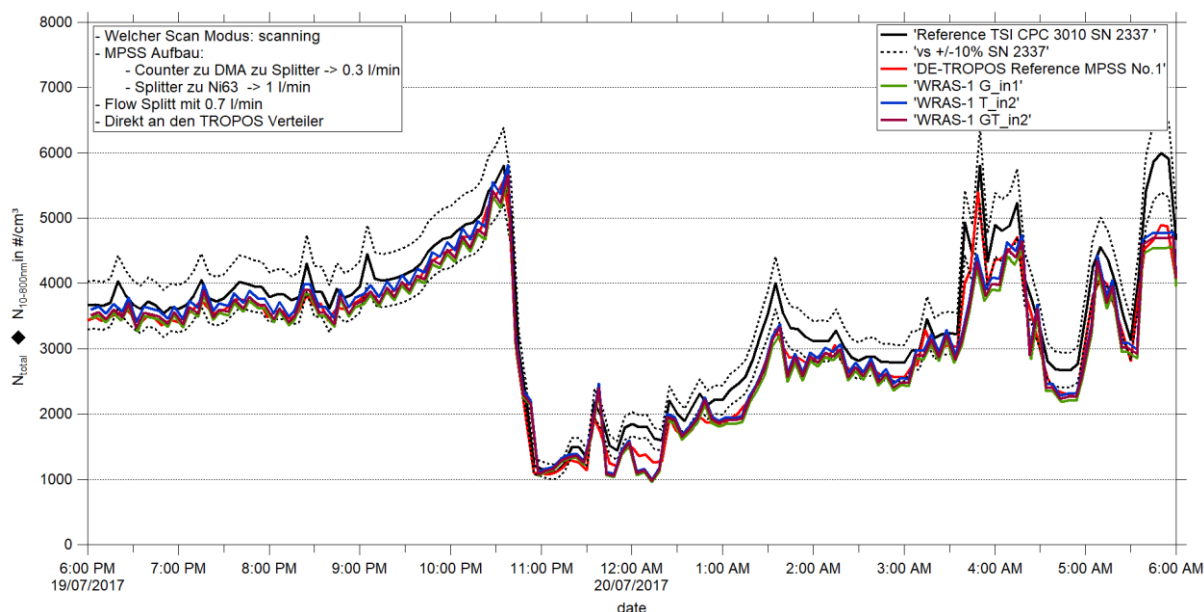
NIGHT: 19. - 20.07.2017

Figure 30: Time series (July 19, 2017 06:00 PM – July 20, 2017 06:00 AM) of the integrated particle number concentration ($N_{10-800nm}$) of the MPSS and total number concentration (N_{total}) of the Reference TSI-CPC Model 3010. The inversion for the candidate was performed using TSI and TROPOS software. Multiple charge correction, internal diffusion losses and CPC flow corrections are included by using different “ini” steps.

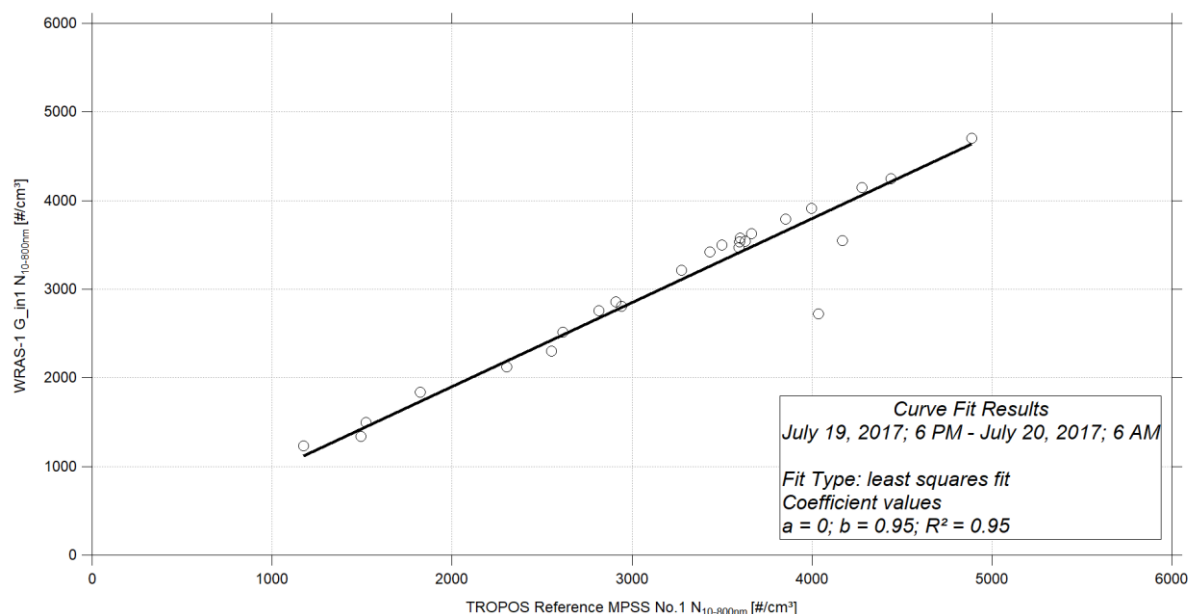


Figure 31: Linear regression between the number concentrations of the TROPOS Reference MPSS No.1 and WRAS-1 G_in1 (July 19, 2017 06:00 PM – July 20, 2017 06:00 AM). Multiple charge correction, internal diffusion losses and CPC flow corrections are included by using different “ini” steps.

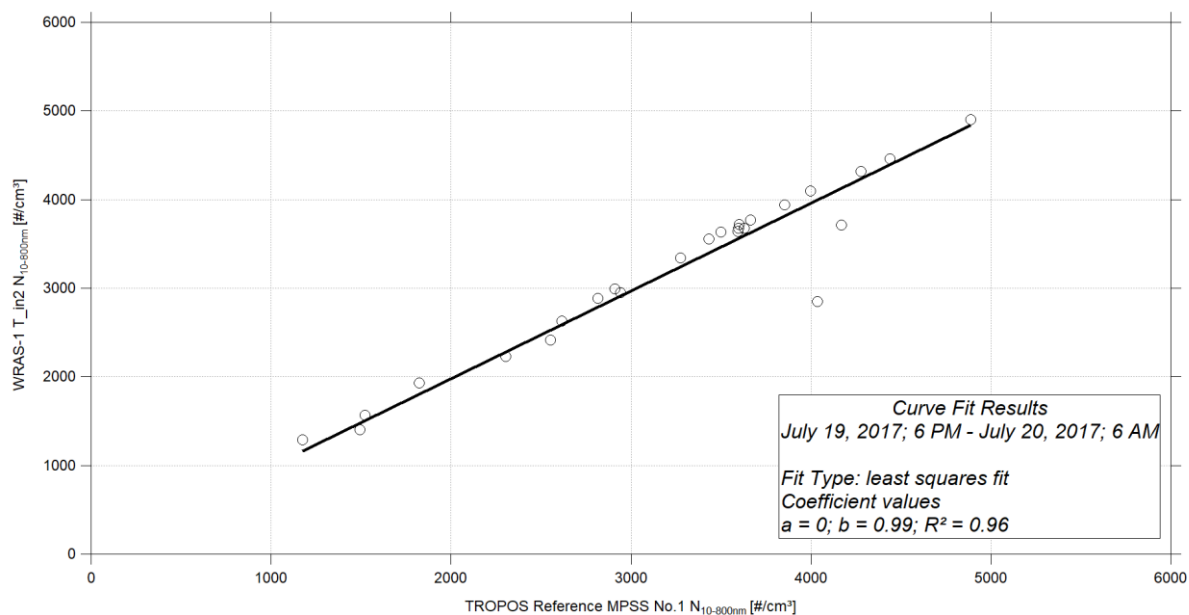


Figure 32: Linear regression between the number concentrations of the TROPOS Reference MPSS No.1 and WRAS-1 T_in2 (July 19, 2017 06:00 PM – July 20, 2017 06:00 AM). Multiple charge correction, internal diffusion losses and CPC flow corrections are included by using different “ini” steps.

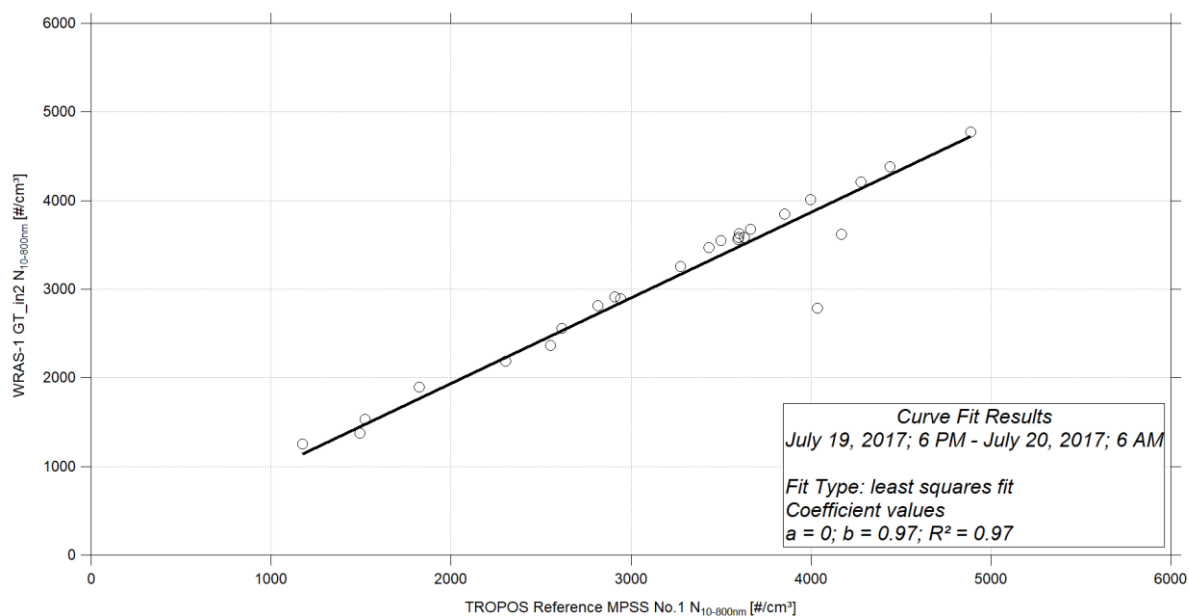


Figure 33: Linear regression between the number concentrations of the TROPOS Reference MPSS No.1 and WRAS-1 GT_in2 (July 19, 2017 06:00 PM – July 20, 2017 06:00 AM). Multiple charge correction, internal diffusion losses and CPC flow corrections are included by using different “ini” steps.

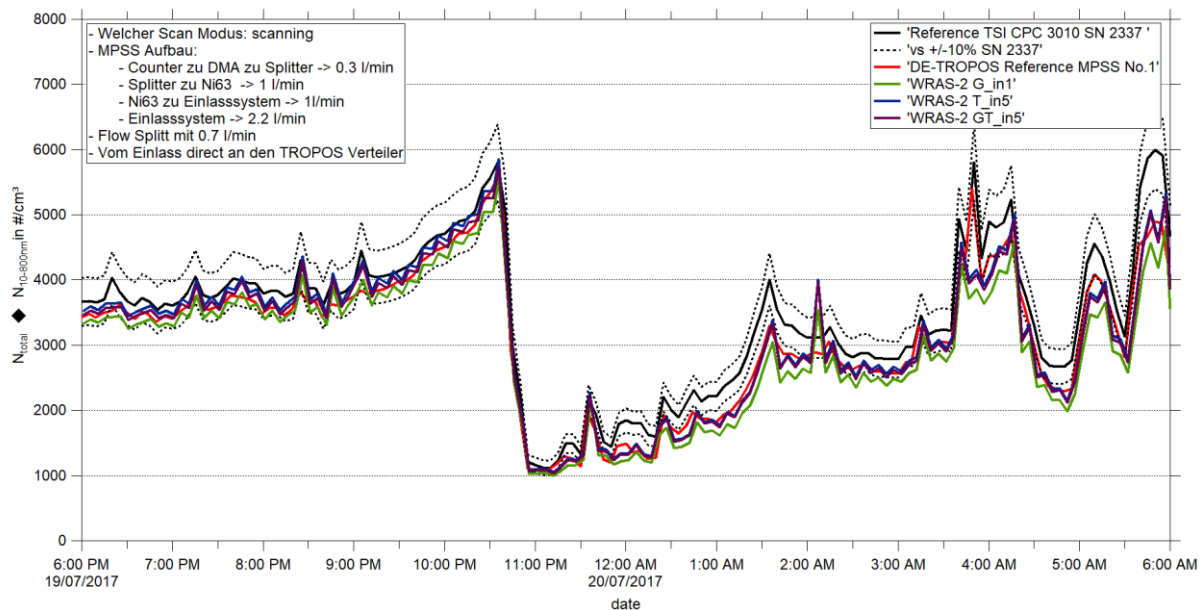


Figure 34: Time series (July 19, 2017 06:00 PM – July 20, 2017 06:00 AM) of the integrated particle number concentration ($N_{10-800nm}$) of the MPSS and total number concentration (N_{total}) of the Reference TSI-CPC Model 3010. The inversion for the candidate was performed using TSI and TROPOS software. Multiple charge correction, internal diffusion losses and CPC flow corrections are included by using different “ini” steps.

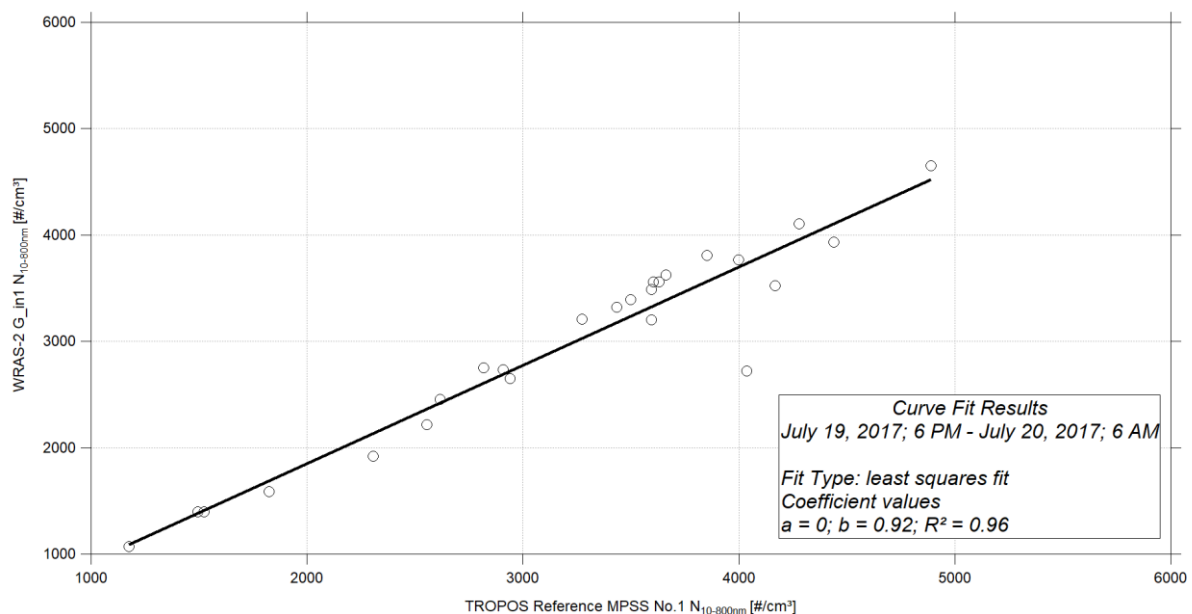


Figure 35: Linear regression between the number concentrations of the TROPOS Reference MPSS No.1 and WRAS-2 G_in1 (July 19, 2017 06:00 PM – July 20, 2017 06:00 AM). Multiple charge correction, internal diffusion losses and CPC flow corrections are included by using different “ini” steps.

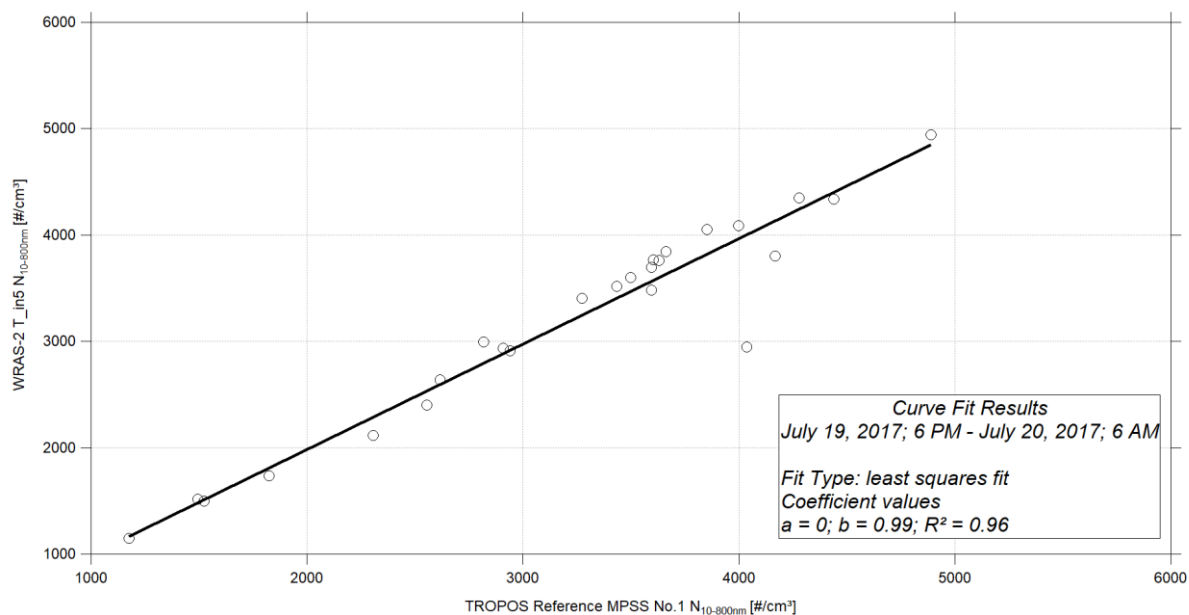


Figure 36: Linear regression between the number concentrations of the TROPOS Reference MPSS No.1 and WRAS-2 T_in5 (July 19, 2017 06:00 PM – July 20, 2017 06:00 AM). Multiple charge correction, internal diffusion losses and CPC flow corrections are included by using different “ini” steps.

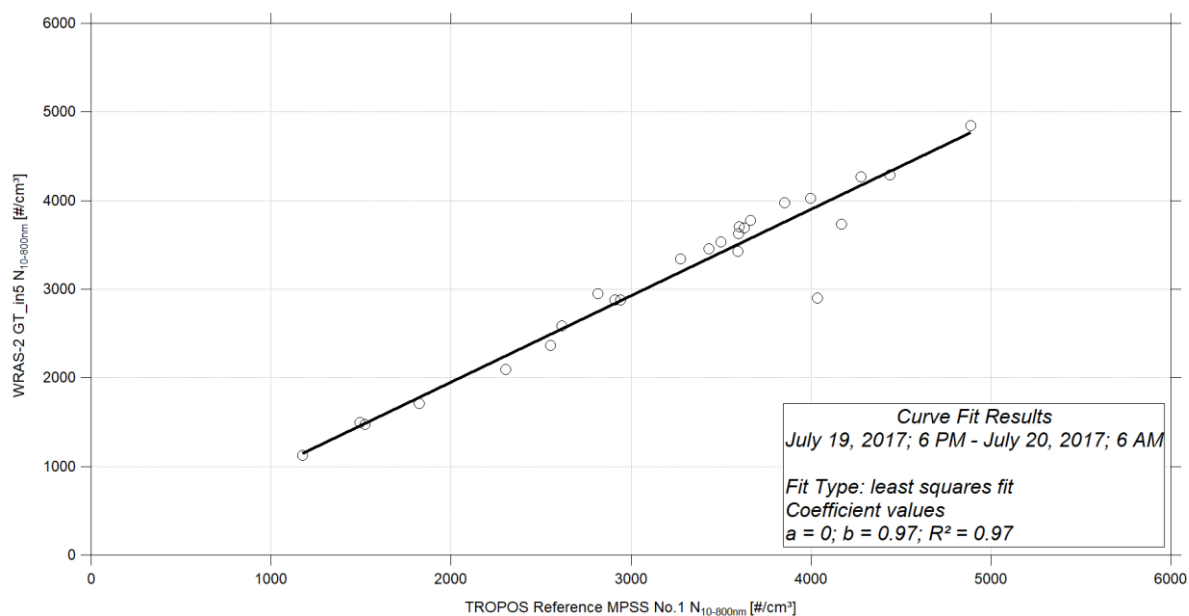


Figure 37: Linear regression between the number concentrations of the TROPOS Reference MPSS No.1 and WRAS-2 GT_in5 (July 19, 2017 06:00 PM – July 20, 2017 06:00 AM). Multiple charge correction, internal diffusion losses and CPC flow corrections are included by using different “ini” steps.

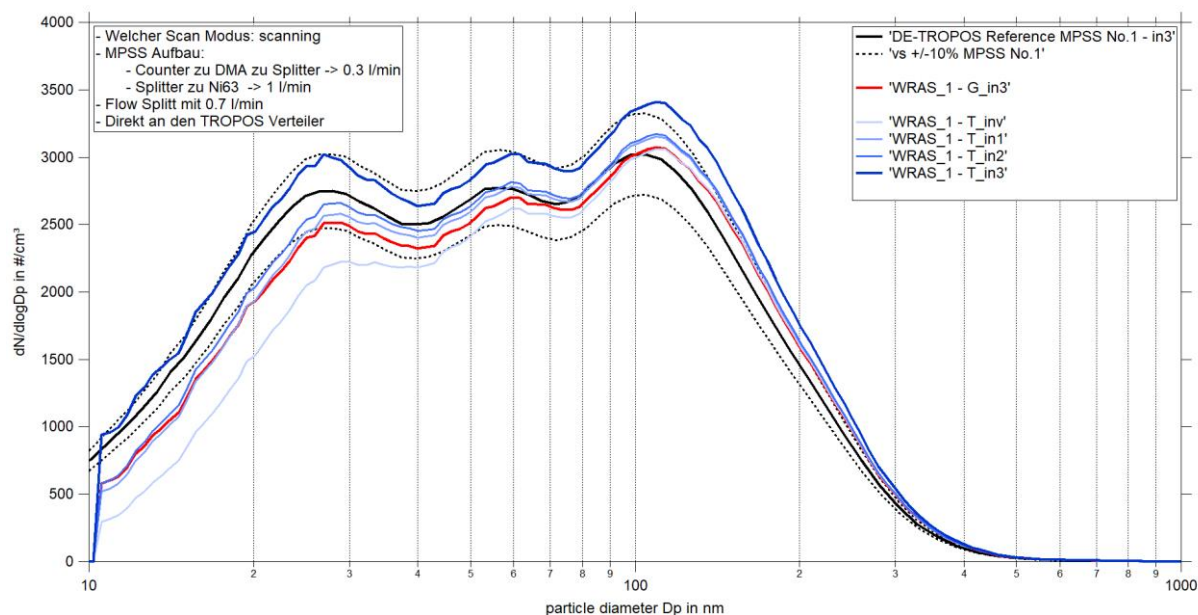


Figure 37: Comparison of mean particle number size distribution of TROPOS Reference MPSS No.1 against WRAS-1 from July 19, 2017 06:00 PM – July 20, 2017 06:00 AM. Multiple charge correction, internal diffusion losses and CPC efficiency are included by using different “ini” steps. Using only TROPOS inversion and corrections.

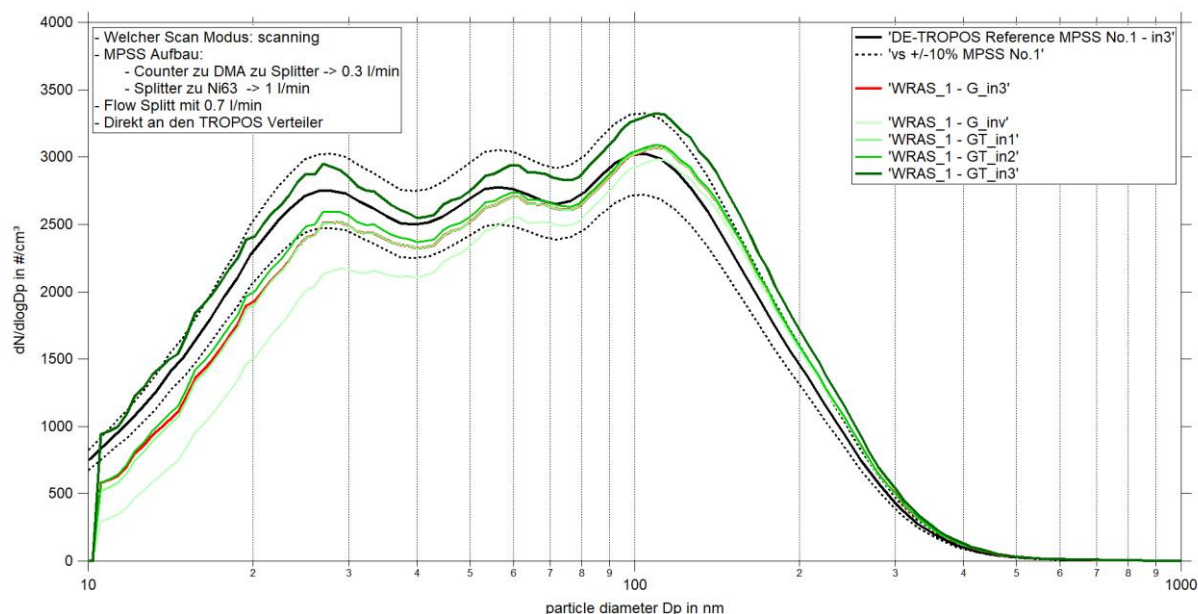


Figure 38: Comparison of mean particle number size distribution of TROPOS Reference MPSS No.1 against WRAS-1 from July 19, 2017 06:00 PM – July 20, 2017 06:00 AM. Multiple charge correction, internal diffusion losses and CPC efficiency are included by using different “ini” steps. Using GRIMM inversion and TROPOS corrections.

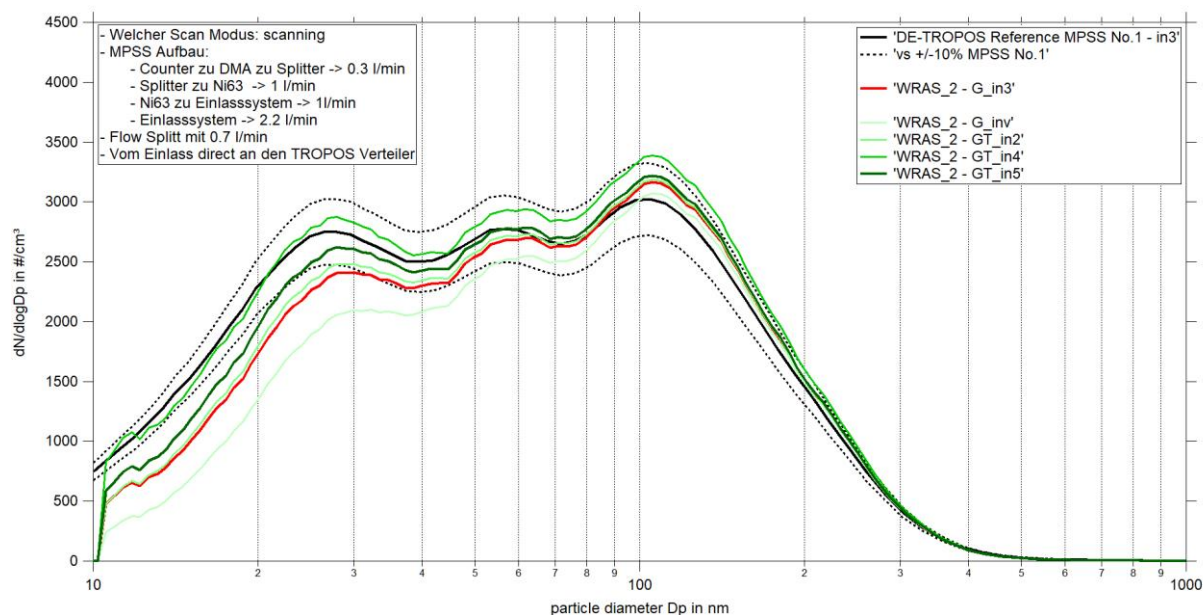


Figure 39: Comparison of mean particle number size distribution of TROPOS Reference MPSS No.1 against WRAS-2 from July 19, 2017 06:00 PM – July 20, 2017 06:00 AM. Multiple charge correction, internal diffusion losses and CPC efficiency are included by using different “ini” steps. Using GRIMM inversion and TROPOS corrections.

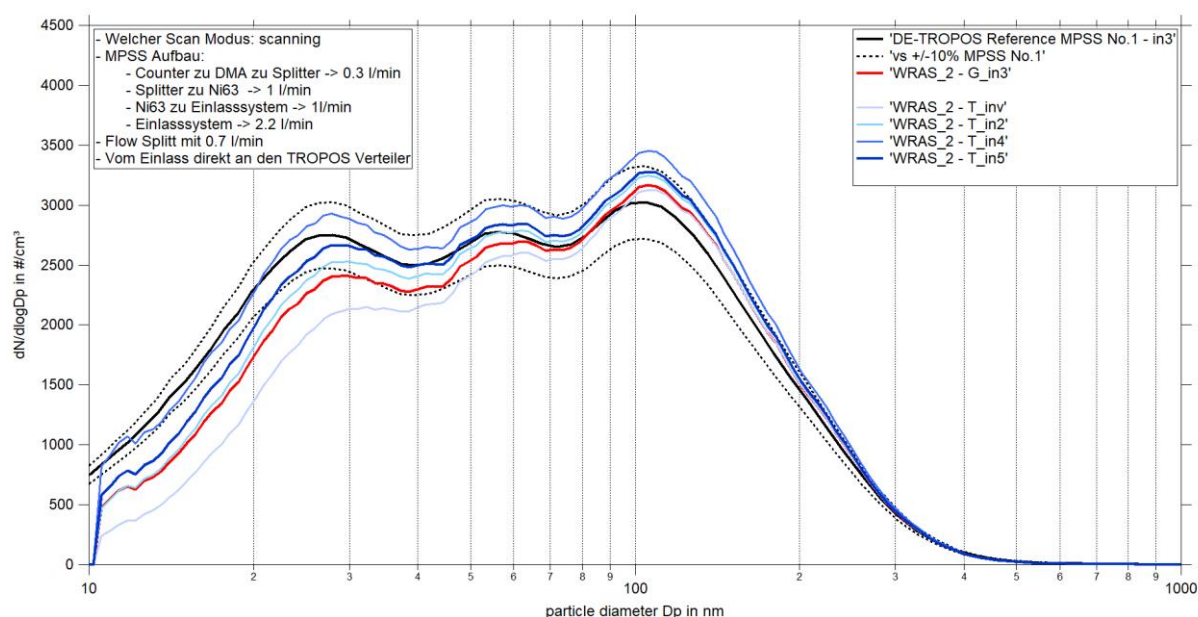


Figure 40: Comparison of mean particle number size distribution of TROPOS Reference MPSS No.1 against WRAS-2 from July 19, 2017 06:00 PM – July 20, 2017 06:00 AM. Multiple charge correction, internal diffusion losses and CPC efficiency are included by using different “ini” steps. Using only TROPOS inversion and corrections.

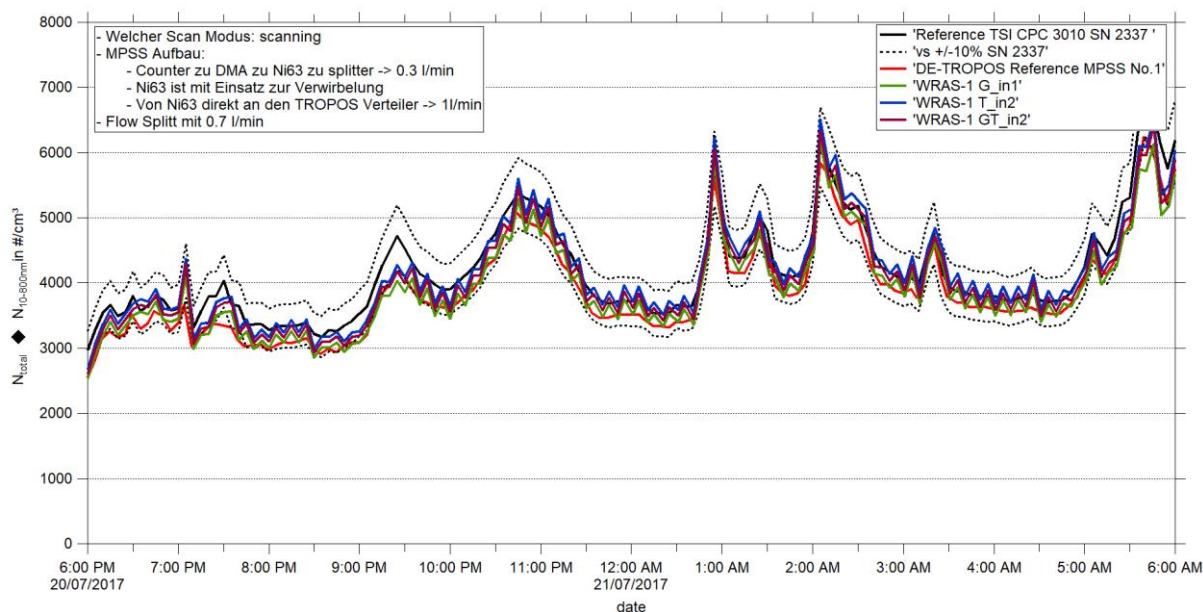
NIGHT: 20. - 21.07.2017

Figure 41: Time series (July 20, 2017 06:00 PM – July 21, 2017 06:00 AM) of the integrated particle number concentration ($N_{10-800nm}$) of the MPSS and total number concentration (N_{total}) of the Reference TSI-CPC Model 3010. The inversion for the candidate was performed using TSI and TROPOS software. Multiple charge correction, internal diffusion losses and CPC flow corrections are included by using different “ini” steps.

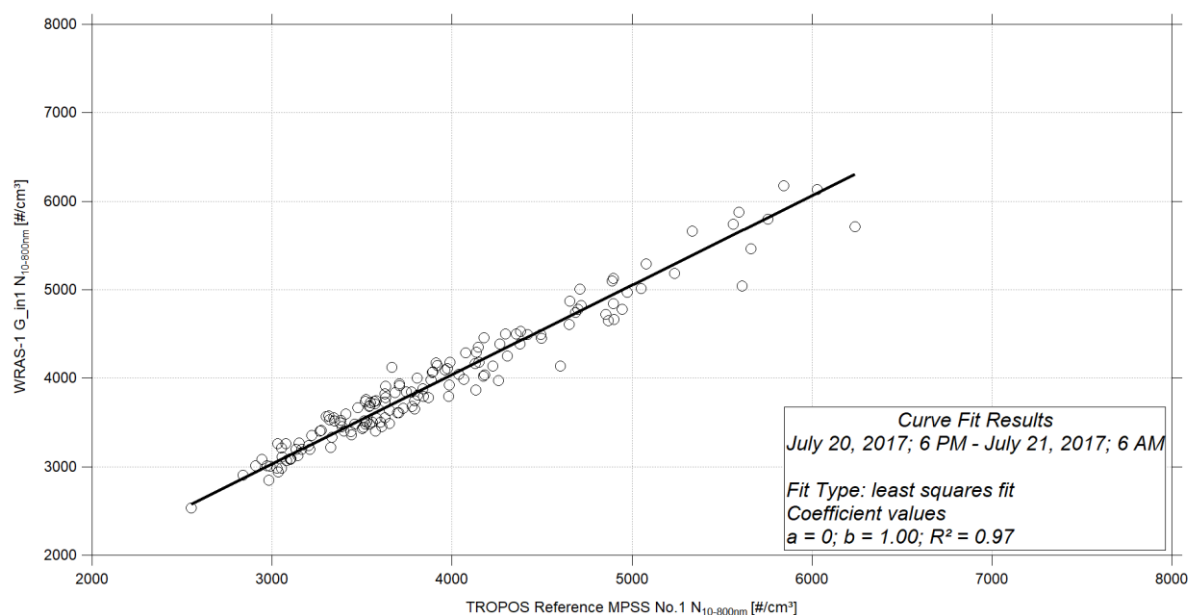


Figure 42: Linear regression between the number concentrations of the TROPOS Reference MPSS No.1 and WRAS-1 G_in1 (July 20, 2017 06:00 PM – July 21, 2017 06:00 AM). Multiple charge correction, internal diffusion losses and CPC flow corrections are included by using different “ini” steps.

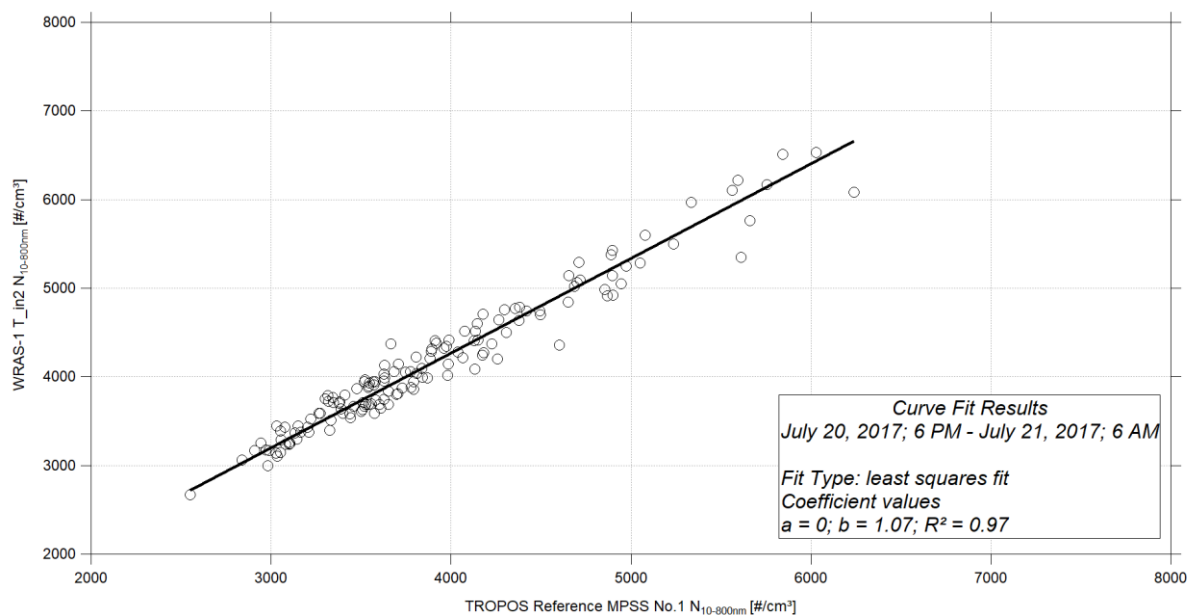


Figure 43: Linear regression between the number concentrations of the TROPOS Reference MPSS No.1 and WRAS-1 T_in2 (July 20, 2017 06:00 PM – July 21, 2017 06:00 AM). Multiple charge correction, internal diffusion losses and CPC flow corrections are included by using different “ini” steps.

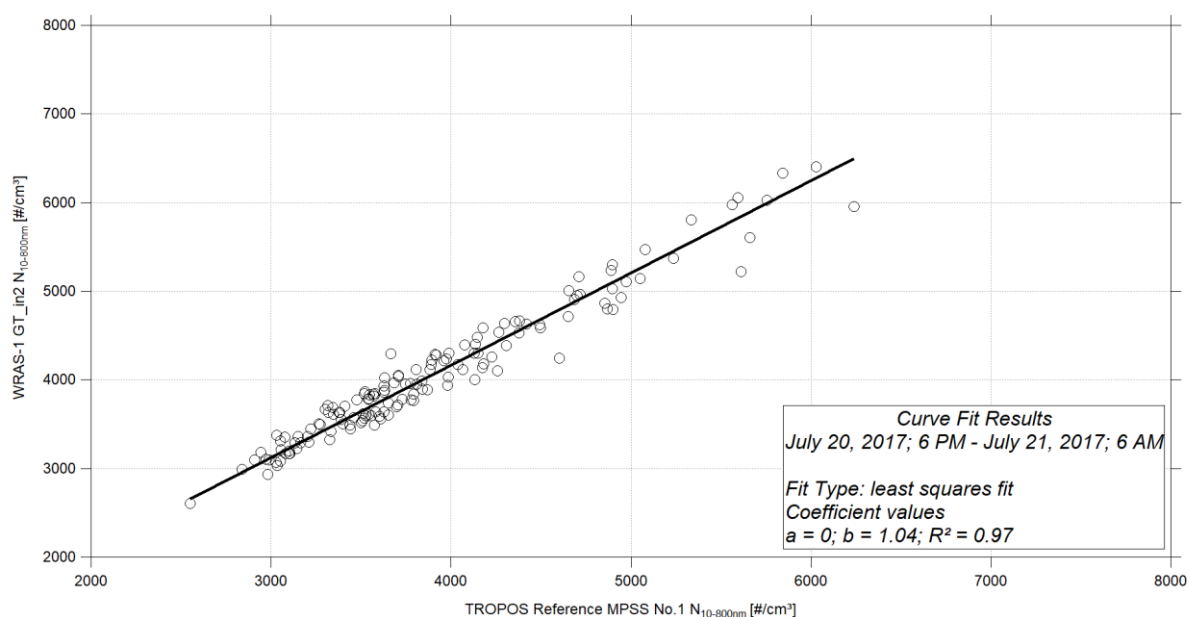


Figure 44: Linear regression between the number concentrations of the TROPOS Reference MPSS No.1 and WRAS-1 GT_in2 (July 20, 2017 06:00 PM – July 21, 2017 06:00 AM). Multiple charge correction, internal diffusion losses and CPC flow corrections are included by using different “ini” steps.

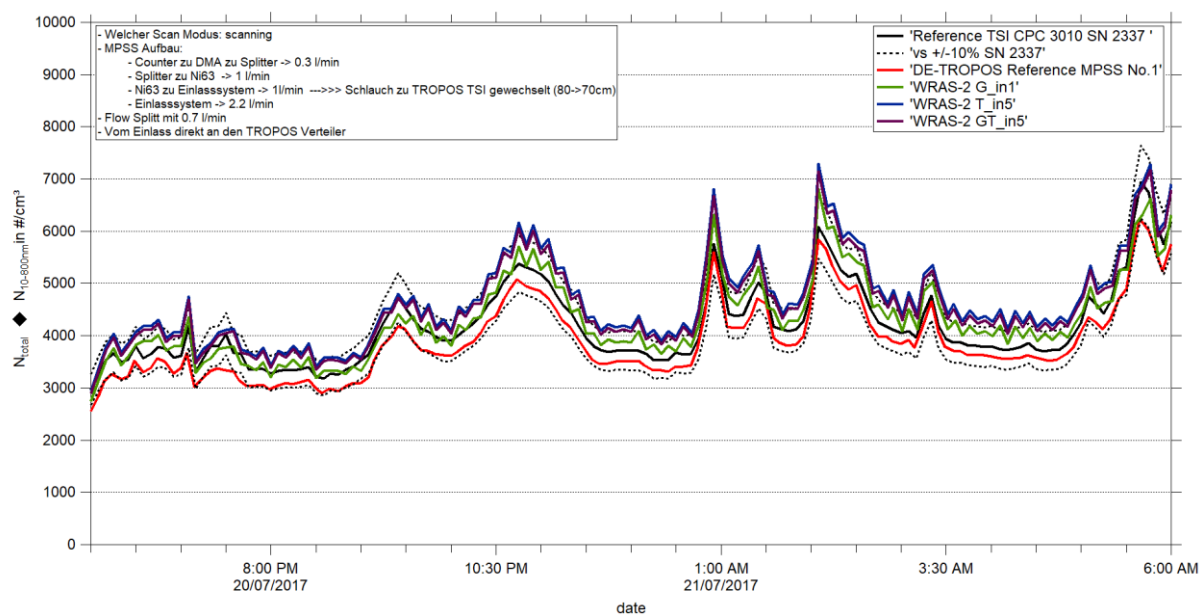


Figure 45: Time series (July 20, 2017 06:00 PM – July 21, 2017 06:00 AM) of the integrated particle number concentration ($N_{10-800nm}$) of the MPSS and total number concentration (N_{total}) of the Reference TSI-CPC Model 3010. The inversion for the candidate was performed using TSI and TROPOS software. Multiple charge correction, internal diffusion losses and CPC flow corrections are included by using different “ini” steps.

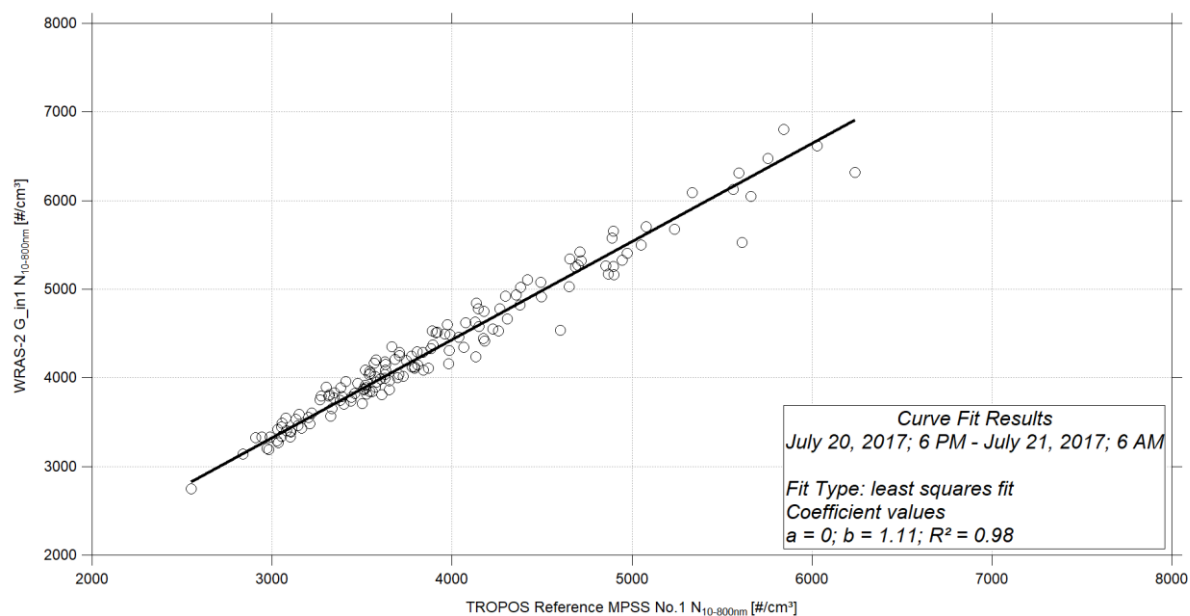


Figure 46: Linear regression between the number concentrations of the TROPOS Reference MPSS No.1 and WRAS-2 G_in1 (July 20, 2017 06:00 PM – July 21, 2017 06:00 AM). Multiple charge correction, internal diffusion losses and CPC flow corrections are included by using different “ini” steps.

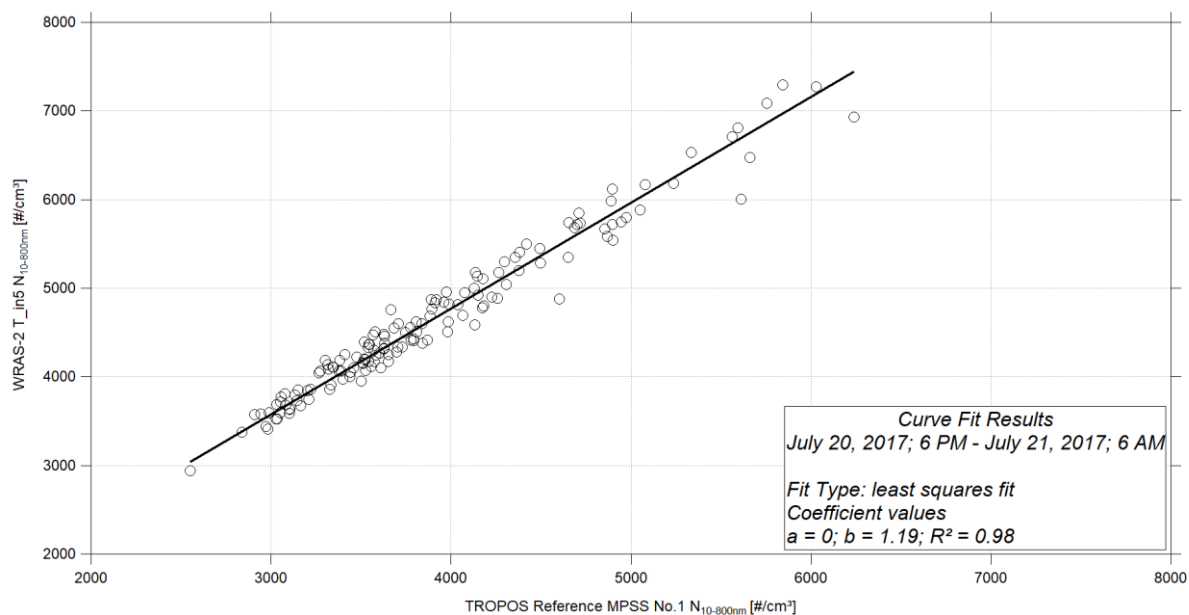


Figure 47: Linear regression between the number concentrations of the TROPOS Reference MPSS No.1 and WRAS-2 T_in5 (July 20, 2017 06:00 PM – July 21, 2017 06:00 AM). Multiple charge correction, internal diffusion losses and CPC flow corrections are included by using different “ini” steps.

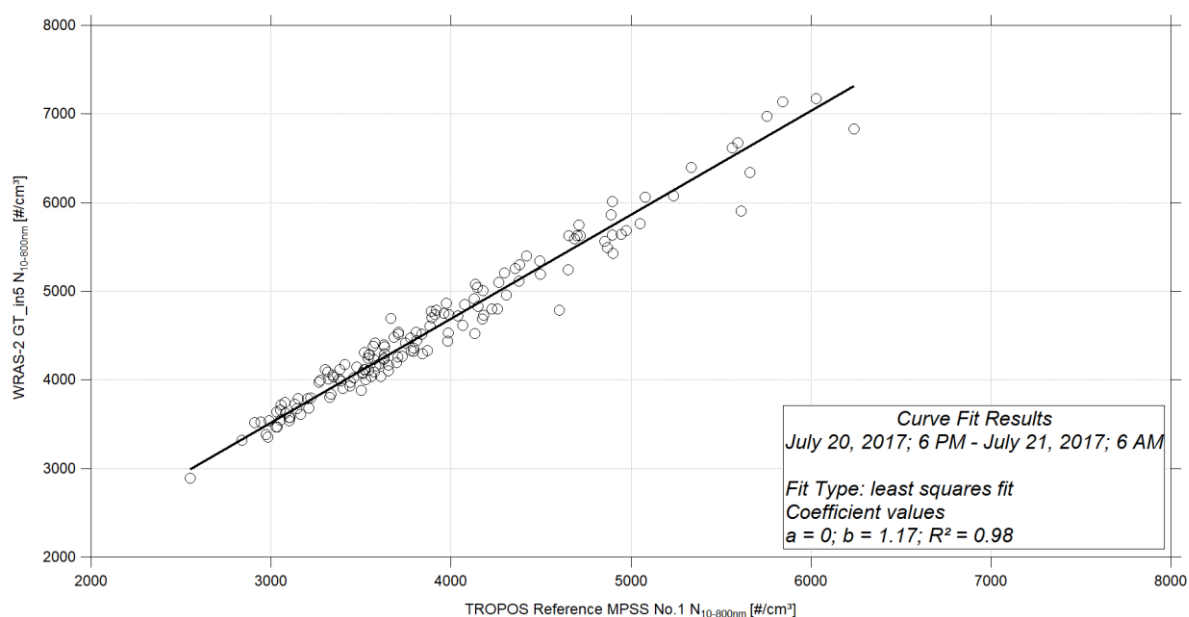


Figure 48: Linear regression between the number concentrations of the TROPOS Reference MPSS No.1 and WRAS-2 GT_in5 (July 20, 2017 06:00 PM – July 21, 2017 06:00 AM). Multiple charge correction, internal diffusion losses and CPC flow corrections are included by using different “ini” steps.

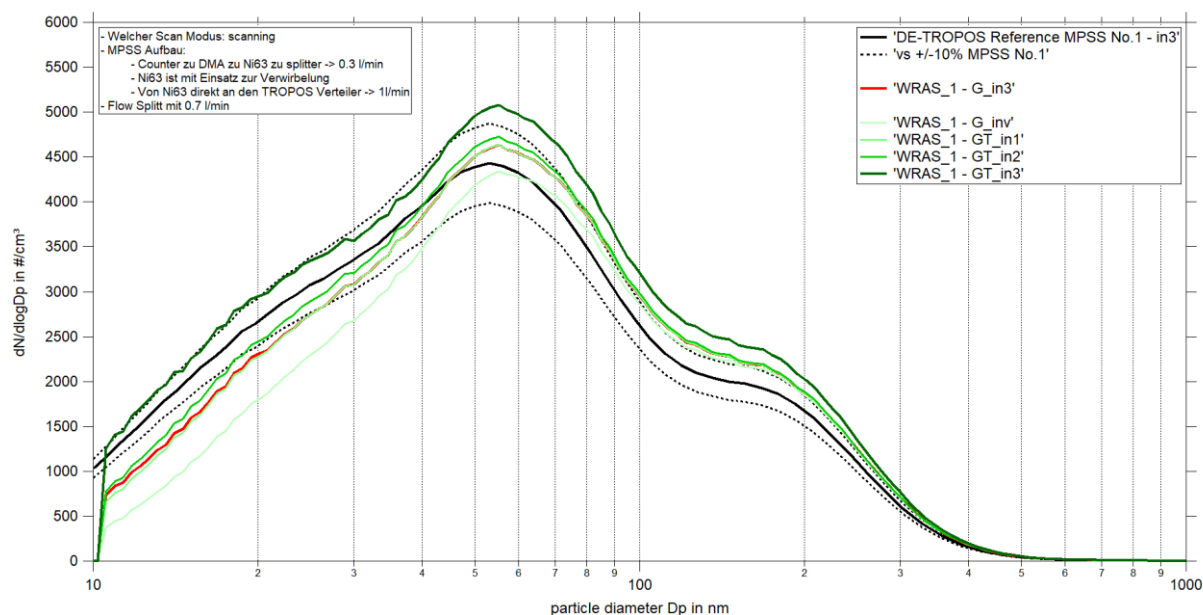


Figure 49: Comparison of mean particle number size distribution of TROPOS Reference MPSS No.1 against WRAS-1 from July 20, 2017 06:00 PM – July 21, 2017 06:00 AM. Multiple charge correction, internal diffusion losses and CPC efficiency are included by using different “ini” steps. Using GRIMM inversion and TROPOS corrections.

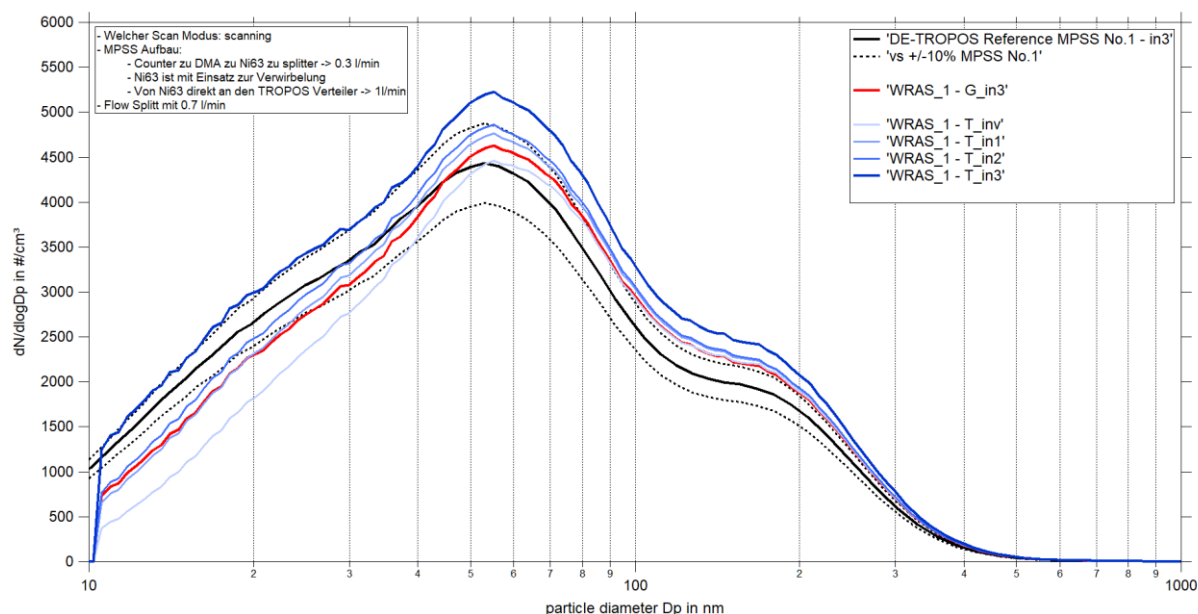


Figure 50: Comparison of mean particle number size distribution of TROPOS Reference MPSS No.1 against WRAS-1 from July 20, 2017 06:00 PM – July 21, 2017 06:00 AM. Multiple charge correction, internal diffusion losses and CPC efficiency are included by using different “ini” steps. Using only TROPOS inversion and corrections.

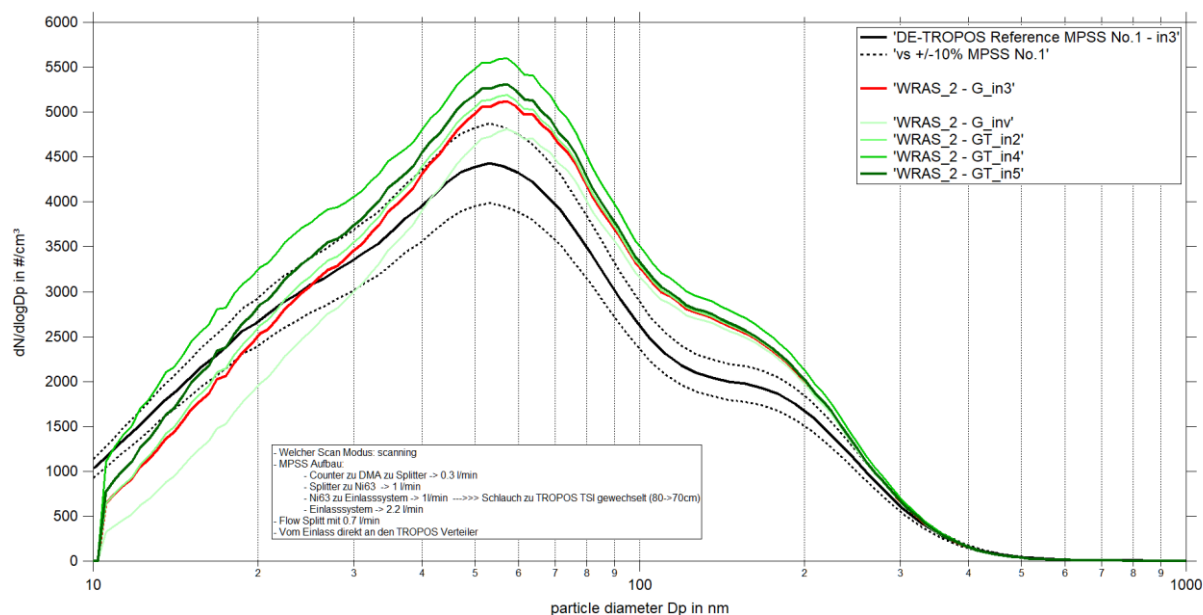


Figure 51: Comparison of mean particle number size distribution of TROPOS Reference MPSS No.1 against WRAS-2 from July 20, 2017 06:00 PM – July 21, 2017 06:00 AM. Multiple charge correction, internal diffusion losses and CPC efficiency are included by using different “ini” steps. Using GRIMM inversion and TROPOS corrections.

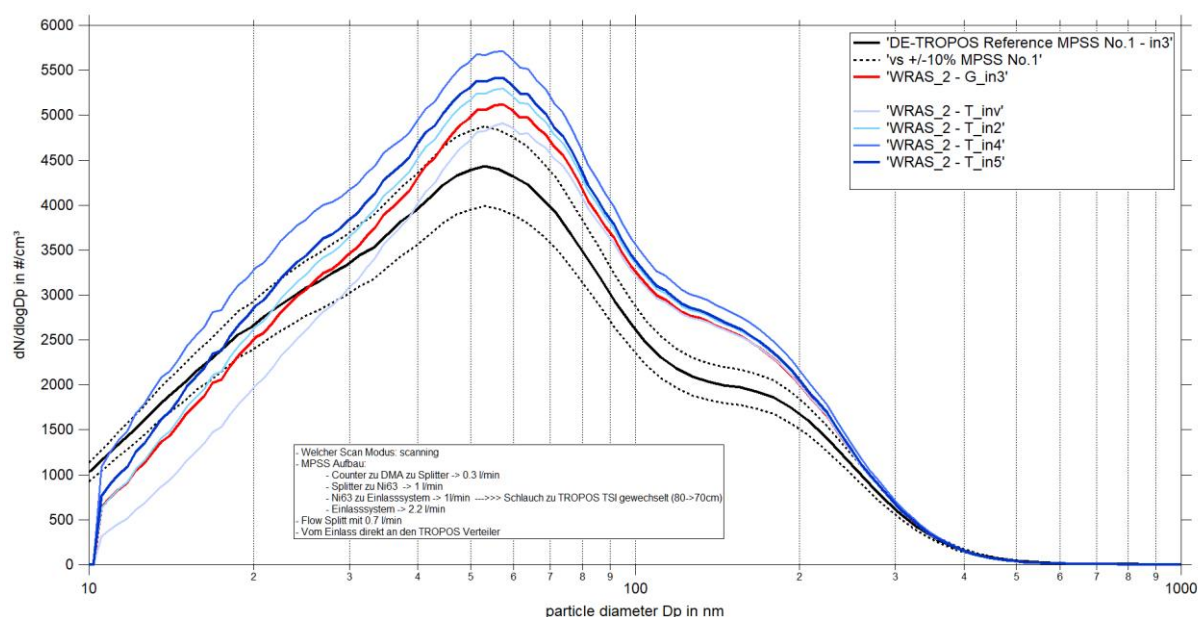


Figure 52: Comparison of mean particle number size distribution of TROPOS Reference MPSS No.1 against WRAS-2 from July 20, 2017 06:00 PM – July 21, 2017 06:00 AM. Multiple charge correction, internal diffusion losses and CPC efficiency are included by using different “ini” steps. Using only TROPOS inversion and corrections.